ELSEVIER

Contents lists available at ScienceDirect

#### Atmospheric Environment: X

journal homepage: www.journals.elsevier.com/atmospheric-environment-x



# Optimisation and validation of Plume Chasing for robust and automated $NO_x$ and particle vehicle emission measurements

Schmidt Christina <sup>a,b</sup>, Carslaw C. David <sup>c</sup>, Farren J. Naomi <sup>c</sup>, Gijlswijk N. René <sup>d</sup>, Knoll Markus <sup>c</sup>, Ligterink E. Norbert <sup>d</sup>, Lollinga Jan Pieter <sup>f</sup>, Pechout Martin <sup>g</sup>, Schmitt Stefan <sup>a,b</sup>, Vojtíšek Michal <sup>g,h</sup>, Vroom Quinn <sup>d</sup>, Pöhler Denis <sup>a,b</sup>

- <sup>a</sup> Institute of Environmental Physics, Heidelberg University, INF 229, Heidelberg, 69120, Germany
- <sup>b</sup> Airyx GmbH, Hans-Bunte-Straße 4, Heidelberg, 69123, Germany
- <sup>c</sup> Wolfson Atmospheric Chemistry Laboratories, University of York, YO10 5DD, York, United Kingdom
- d Department of Sustainable Transport and Logistics, TNO, Anna van Buerenplein 1, The Hague, 2595, The Netherlands
- e Institute of Electrical Measurement and Sensor Systems, Graz University of Technology, Inffeldgasse 33/I, Graz, 8010, Austria
- <sup>f</sup> Department of Environmental Modelling, Sensing & Analysis, TNO, Utrecht, 3584, The Netherlands
- § Department of Vehicles and Ground Transport, Czech University of Life Sciences, Kamycka 129, Praha-Suchdol, 165 21, Czech Republic
- h Department of Automotive, Combustion Engine and Railway Engineering, Czech Technical University of Prague, Technicka 4, Prague, 166 07, Czech Republic

#### ARTICLE INFO

# Keywords: Plume Chasing Remote emission sensing Real-world vehicle emissions High-emitter identification Interfering emission sources NO<sub>v</sub> and PM measurements

#### ABSTRACT

High-emitting vehicles comprise a small proportion (< 20%) of the vehicle fleet, yet are responsible for the majority (> 50%) of vehicle emissions. Plume Chasing is a reliable, high-precision measurement technique that derives emissions without interfering with the vehicle being tested. Its characteristics make it well suited for high emitter identification. In this study, the influence of several Plume Chasing measurement and data processing methods on the results of derived on-road  $NO_x$  and particle fuel-specific emission factors are investigated. A range of vehicles, representative of a common vehicle fleet, were tested under different driving conditions on a test track. The derived results were evaluated against on-board SEMS (Smart Emission Measurement System) emission measurements. We found that one of the best performing Plume Chasing data processing methods is based on the use of a rolling minimum for background determination. The average absolute deviation of the determined  $NO_x/CO_2$  emission ratios from the reference was  $-0.2(46)\,\mathrm{ppm}/\%$  for the heavy duty vehicle and  $0.3(29)\,\mathrm{ppm}/\%$  for the light duty vehicles tested. The methods were easy to automate and suitable for high emitter detection and quantification of emissions from two-wheeled vehicles. Inaccurate emission factors derived from Plume Chasing measurements occurred only in situations when emissions were significantly influenced by a strong plume from vehicles driving directly ahead of the vehicle of interest.

#### 1. Introduction

Nitrogen Oxides ( $\mathrm{NO_x}$ ) and particulate matter (PM) emissions from vehicles are major contributors to poor air quality in urban areas. The vehicle emissions are regulated by the Euro emission standard (e.g. heavy duty vehicles (HDVs)  $\mathrm{NO_x}$  Euro V:  $2000\,\mathrm{mg/kWh}$ , Euro VI:  $460\,\mathrm{mg/kWh}$ ). In order to comply with increasingly stringent emission standards, vehicles are applying technologies like Exhaust Gas Re-circulation (EGR), Selective Catalytic Reduction (SCR), or Diesel Particulate Filters (DPFs). Throughout their lifespan, vehicles are often not properly maintained or even tampered, resulting in significantly higher emissions. Several studies have demonstrated that these highemitters are responsible for the major share of emissions (Olin et al., 2023; Zhou et al., 2020; Vojtisek-Lom et al., 2020a; Boveroux et al.,

2019; Burtscher et al., 2019). Zhou et al. (2020) found that the highest 10% of HDVs were responsible for 44–70% of total emissions, depending on the pollutant. Olin et al. (2023) found that the most emitting 20% of vehicles contribute to over 80% of particle number (PN) emissions. With the reduction in emissions from new vehicles due to more stringent regulations, the contribution of high-emitters to total emissions is likely to increase further. Therefore, it is crucial to monitor, identify and remove or repair such high-emitters, in order to significantly improve the overall air quality. Several remote emission sensing techniques such as Plume Chasing, open-path cross-road Remote Sensing (Bishop et al., 1989) or Point Sampling (Hansen and Rosen, 1990) are well capable of quantifying real-world driving vehicle

<sup>\*</sup> Corresponding author at: Institute of Environmental Physics, Heidelberg University, INF 229, Heidelberg, 69120, Germany. E-mail address: cschmidt@iup.uni-heidelberg.de (C. Schmidt).

emissions and have been further developed in recent years (Ropkins et al., 2017; Knoll et al., 2024). The main advantages of Plume Chasing over other remote sensing methods are that the emission is not measured at a snapshot, but averaged over a longer period of time (typically several minutes), and that Plume Chasing cannot be avoided by drivers by decelerating through the measurement point or changing routes, as it is mobile and can be very easily relocated if the information about the ongoing measurement is circulated among drivers. This gives a more representative emission value and avoids errors for specific test conditions. Plume Chasing has proven to be perfectly suitable for highemitter identification (see for instance Janssen and Hagberg, 2020; Pöhler, 2021).

Various data processing methods for Plume Chasing have been reported in the literature, which can be separated into regression-based or integration-based approaches. The 'regression' approach (linear, robust or rolling regression) derives emissions from the regression slope of the pollutant under consideration (e.g.  $NO_x$  or PM) versus  $CO_2$  (Zavala et al., 2006; Vojtisek-Lom et al., 2020a; Olin et al., 2023; Farren et al., 2023). The 'integration' approach, on the other hand, averages the background (BG) corrected time series of pollutant and  $CO_2$  individually and then calculates an emission ratio (Hansen and Rosen, 1990). For the latter approach, the BG concentrations are in most cases determined either from a time interval in which there are no other emission sources, or from a rolling time window in which the BG is searched (Ježek et al., 2015; Wen et al., 2019; Pöhler et al., 2020). Approaches for vehicles without  $CO_2$  emissions can be found in Leinonen et al. (2023).

For HDVs, several validation studies comparing the Plume Chasing technique with the established PEMS have already previously shown excellent agreement between the observed emission values (e.g. Roth, 2018; Janssen and Hagberg, 2020; Wang et al., 2020; Tong et al., 2022; Xiang et al., 2023). However, there are only few validation studies with light duty vehicles (LDVs) (e.g. Pöhler et al., 2020; Simonen et al., 2019; Ježek et al., 2015) and to our knowledge none with 2-wheeled vehicles. Most of the Plume Chasing validation studies discussed in the literature have been carried out in environments with as little influence as possible from interfering emission sources (e.g. on test tracks Ježek et al., 2015 or on low-traffic roads Wang et al., 2020; Tong et al., 2022).

We present an extensive validation study done within the framework of the EU project CARES (City Air Remote Emission Sensing) (Horizon, 2020), comparing different data processing methods and influences on the Plume Chasing method. Comparisons with on-board measurements of Smart Emission Measurement Systems (SEMS) for NOx, Mini Portable Emission Measurement Systems (Mini-PEMS) for Nitrogen Oxide (NO) and PN instruments measuring directly at the tailpipe were performed. The study examined emissions by simulating a typical vehicle fleet consisting of one HDV, three LDVs and two 2wheeled vehicles (motorcycle/scooter). We investigate the influence of dense traffic on the Plume Chasing measurements: measurements are taken on a test track under controlled convoy driving conditions, with vehicles of very different emission levels driving at different vehicle headways and in different driving orders, simulating different driving situations. The influence of high-emitting vehicles driving close to lowemitting vehicles is also investigated. The ability of the Plume Chasing system to identify vehicles with a tampered emission reduction system under different driving conditions is shown. In addition, real traffic measurements on busy roads were carried out with one of the LDVs studied, including on-board measurements of NOx and PN.

#### 2. Methods

#### 2.1. Instrumental setup

The Plume Chasing method uses a measurement vehicle equipped with various instruments (e.g. gas – always including  $\rm CO_2$  – and particle

analysers) to measure the emissions of vehicles (Fig. 1). The measurement vehicle follows the vehicle under study at a safe distance (about 2-second gap). The sampled air from the diluted exhaust plume is analysed by these instruments in real-time. Assuming that the ratio between pollutant and CO2 remains unchanged by dilution and that chemical degradation is negligible on the short timescale, the specific emissions can be calculated based on the ratio in the sampled air. Fuel-based (g/kg fuel), distance based (g/km) or energy based (g/kWh) emission factors can be calculated from the pollutant (e.g. NO<sub>x</sub>) to CO<sub>2</sub> ratio, using assumptions of the CO<sub>2</sub> emissions (engine efficiency). In this study, a comprehensive Plume Chasing setup was chosen for research purposes to further optimise the Plume Chasing measurement technique by comparing different instruments and methods. Much simpler setups can be used for routine Plume Chasing and a single ICAD (Iterative CAvity enhanced DOAS) analyser (Airyx GmbH, Horbanski et al., 2019) can be sufficient for e.g. investigation of NO<sub>x</sub> and CO<sub>2</sub> emissions (Janssen and Hagberg, 2020).

A VW transporter, type T5 TDI 4 motion (high top) from TNO (Utrecht, the Netherlands) was used as the measurement vehicle (Fig. B.13). An ultrasonic anemometer measured the wind speed and direction on the roof of the measurement vehicle, while a radar determined the distance to the chased vehicle. A dashboard camera captured images of the chase to provide additional information for interpreting the data collected. To analyse the gases NO<sub>x</sub>, NO<sub>2</sub> and CO<sub>2</sub> of the plume signal, an ICAD-NOx-150DE-M instrument (Airyx GmbH) was installed and a second CO2 measurement was realised with a LI-COR 7000 sensor. PN concentrations in the plume signal were analysed by a Condensation Particle Counter (CPC) and a TEN AEM Particle Counter (TEN). The CPC measured total PN with a particle diameter larger than 2.5 nm (PN<sub>2.5</sub>, 50 % counting efficiency at 2.5 nm), the TEN non-volatile PN larger than 23 nm (PN23). In addition, a Scanning Mobility Particle Sizer (SMPS) measured the PN concentration with an electrical mobility diameter of around 90 nm (PN@90). A second ICAD-NOx-150DE-M instrument was used for additional background measurements with an additional inlet installed on the roof of the vehicle to test an alternative Plume Chasing measurement approach. The different instruments for CO2 and PM measurements were used to investigate which of them are the most suitable for this application. The ICAD analyser was selected as the NO<sub>x</sub> instrument since it has been shown in test measurements prior to this study to be reliable for Plume Chasing applications and better suited than other techniques such as Chemiluminescence Detection (CLD). The instruments used allow fast and simple measurements with high accuracy and a wide measurement range with a low power consumption (Table 1), ideal for such mobile measurements. Further details of the instruments installed are given in Table 1.

Teflon tubing was used for gas sampling and stainless steel together with conductive silicon tubing for PM. The inlet sampling position was approximately 30 cm above the road and 10 cm in front of the bumper of the van (Fig. B.13, right). Two inlets were used on the left and right (150 cm apart) and merged into a central sampling line before reaching the instruments. This arrangement was found to give a more reliable measurement of the plume, being less sensitive to the position of the exhaust on the chased vehicles and also to meteorological effects such as crosswinds. For an alternative BG measurement approach (Section 2.5.3), a gas inlet was installed approximately 40 cm above the road surface. The described inlet positions and the choice of instruments were optimised in previous experiments during the CARES project.

#### 2.2. Measurement procedure

#### 2.2.1. Test track experiments

In June 2021, controlled Plume Chasing measurements were carried out on different types of vehicles (Table 2) representative of a common vehicle fleet. During 5 days on the test track (2.8 km long, circuit;

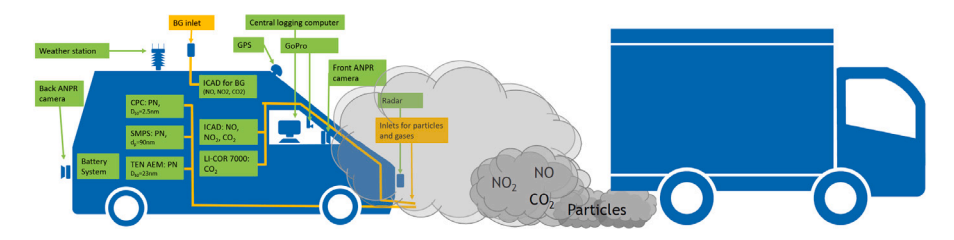


Fig. 1. Schematic of the Plume Chasing method with a comprehensive emission measurement setup.

Table 1
Instruments installed in the Plume Chasing vehicle (VW transporter T5 from TNO).

Parameter	Instrument	Measurement range	Accuracy	Power
NO <sub>x</sub> , NO <sub>2</sub> ,	ICAD-NO <sub>v</sub> -150DE-M	0 5000 ppb	0.8 ppb (1σ @ 1 s)	< 30 W
$CO_2$	ICAD-NO <sub>x</sub> -150DE-M	02000 ppm	1% slope $+ < 20$ ppm abs.	$< 2 \mathrm{W}$
CO <sub>2</sub>	LI-COR 7000	0 3000 ppm	1 % nominally	$< 40 \mathrm{W}$
PN <sub>2.5</sub>	TSI 3776 CPC	up to $3 \cdot 10^5 \text{ #/cm}^3$	$\pm 10\% < 300.000 \text{ #/cm}^3$	< 335 W
$(D_{50} = 2.5 \mathrm{nm})$				
PN@90	SMPS (Electrostatic Classifier	up to $5 \cdot 10^4 \text{ #/cm}^3$	$\pm 10\% < 300.000 \text{ #/cm}^3$	< 535 W
$(d_n = 90  \text{nm})$	3082 and TSI 3775 CPC)	photometric mode up to 107		
$PN_{23}$	TEN AEM particle counter	$5 \cdot 10^3 \dots 5 \cdot 10^6 \text{ #/cm}^3$	$25.000  \text{#/cm}^3 \text{ of } \pm 25  \%$	$< 100 \mathrm{W}$
$(D_{50} = 23 \mathrm{nm})$				
Location, Speed	Navilock Multi GNSS u-blox 8		2.5 m CEP	< 0.2 W
Number Plate	ARVOO ANPR camera			
	(DUO12-35/25m35/25c780)			
Distance	Continental ARS 308 radar	0.25200 m	1.5 % @ > 1 m	< 7 W
Wind speed,	Vaisala WTX530 series, model	0 60 m/s	3 %@10 m/s	< 9.7 W
Wind direction	536	0 360°	3.0°@10 m/s	



Fig. 2. Selection of test vehicles at RDW test track, Lelystad, the Netherlands, chasing vehicle at 4th position. Motorcycle and Scooter not shown in the picture.

 Table 2

 Technical vehicle information for the six test vehicles investigated in this study.

Category	Brand	Туре	Fuel type	Euro class
N3	Ford	F-Max Truck	Diesel	VI
N1	VW	Caddy	Diesel	6
M1	VW	Transporter	Diesel	6
M1	VW	Touran	Gasoline	5
L3	Yamaha	MT-07 Motorcycle	Gasoline	5
L3	Yamaha	NMAX Scooter	Gasoline	5

Fig. 2) of the Rijksdienst voor het Wegverkeer Test Centre Lelystad, the Netherlands, three remote emission sensing techniques were tested and compared: Plume Chasing, open-path cross-road Remote Sensing (Opus RSE) and Point Sampling (Farren et al., 2022a,b). The Opus remote sensing device and Point Sampling equipment were deployed on a fixed point of the test track, while the Plume Chasing vehicle chased the test vehicles on the test track. Some of the test vehicles were equipped with on-board equipment (SEMS, Mini-PEMS and a NanoMet3) for measurement validation purposes. In 21 different sessions each vehicle was followed by the Plume Chasing vehicle for at least one lap (about 2.8 km) before switching to the next vehicle. The distance to the chased vehicle was kept constant at between 8 and 35 m, depending on the vehicle speed. In the different sessions, the emission control systems (SCR of the Ford truck, the VW Caddy and VW Transporter; DPF of the VW Caddy) of some of the test vehicles were activated and deactivated in a blind comparison experiment, resulting in a mixture of low and

high emissions (see Section 3). SCR tampering was achieved by deactivating the AdBlue dosing by manipulating the vehicle's SCR software in the case of the truck and by unplugging the diesel exhaust fluid dosing injector on the VW Caddy and VW Transporter. The DPF was tampered with a small bypass line of approx. 8 mm around the DPF that could be activated and deactivated with a manual valve. In addition, the driving conditions (speed, distance between the vehicles or their driving order) were varied to investigate strengths and weaknesses of the different remote emission sensing techniques in identifying high and low emitters. The test vehicles drove either as single vehicles with a large distance (> 50 m) to the next vehicle or in 'convoys'. The measurement data is flagged as convoy and non-convoy to be able to investigate the influence of other nearby vehicles on the measurements. In the case of convoy driving, the first vehicle was not assigned to the convoy driving as there was no other plume from a vehicle in front affecting the measurements. During the test track measurements there was no rain and the wind speed ranged from 6 to 11 m/s (daily average) (Table A.6). An example time series of time-aligned NO<sub>x</sub> and CO<sub>2</sub> data from both SEMS and Plume Chasing is shown in Fig. E.17, along with information on speed and distance to the chased vehicle. For more information on the test track experiments, see Farren et al. (2022a,b, 2023).

#### 2.2.2. Real traffic experiments

Plume Chasing measurements of one of the test vehicles (the VW Caddy) in real traffic conditions were performed on 17th and 18th of

June 2021, each for approximately 1 h and 40 min in different driving environments (Fig. A.12 in the Appendix). We divided the driving environment in two sections, urban/suburban/rural and highway. Traffic was lower in the urban/suburban/rural environment compared to the highway. However, in the urban/suburban/rural environment there were still many other vehicles and emission sources present. For onboard  $\mathrm{NO}_x$  and  $\mathrm{CO}_2$  measurements a SEMS was installed. In addition, on the 18th of June 2021, the TEN from the Plume Chasing vehicle was installed in the VW Caddy for  $\mathrm{PN}_{23}$  on-board measurements. The VW Caddy was also tampered (SCR+DPF), but no significant differences in emissions were observed in reference on-board measurements so that no separation is performed for tampered and non-tampered data in the data analysis. Why the tampering was not working is unclear, but the tampering procedure was improved for the following test track measurements.

#### 2.3. Data analysis

The raw data was first cleaned of corrupted and duplicate data within the datasets and then time-shifted to account for the residence time in the tubing and the time shifts between the respective instruments. Then the signals were smoothed with Gaussian filters with suitable widths in time to account for the different response functions of the instruments compared to the ICAD  $\rm CO_2$  sensor. To determine the residence time in the tubing and the parameters for the smoothing, short pollution peaks at the sampling inlets from a lighter were regularly used as a reference. Cross-correlation was used to determine the time shift between the different pollutants, where the time shift is the lag corresponding to the maximum cross-correlation coefficient.

In general, we want to determine the average emissions  $E_X$  of pollutant X from a vehicle. Where X denotes any pollutant of interest (i.e.  $NO_X$  and PM) emitted simultaneously to  $CO_2$ . If the pollutant to  $CO_2$  ratio  $R_E$  can be determined, then for known average  $CO_2$  emissions ( $E_{CO_2}$ ), the average emissions of pollutant X can be calculated using Eq. (1).

$$R_E = \frac{E_X}{E_{CO_2}} \tag{1}$$

 $\rm E_{\rm CO_2}$  of HDVs per kWh can be calculated from the well-known correlation between the diesel energy content in kWh/l and its emission of  $\rm CO_2/l$  (i.e. the carbon content of a litre of Diesel fuel). The diesel energy content is additionally multiplied by the efficiency of the diesel engine (here we use 40 %) to consider only the energy available for HDV motion. The average  $\rm CO_2$  emission per km of a LDV is known as its type-approval  $\rm CO_2$  emission, or more precise from real driving  $\rm CO_2$  emission databases. In most cases it is sufficient for this study to determine the emission ratio  $R_E$  from the measurements.

The emission ratio  $R_E$  of the diluted compounds can be determined by different Plume Chasing data processing methods. All methods assume that  $\mathrm{CO}_2$  and all pollutants are diluted equally and that there is no chemical loss of species X between exhaust pipe and the sampling inlet. Due to turbulence in the emission plume, a separation of pollutant X and  $\mathrm{CO}_2$  is not to be expected. Since  $\mathrm{NO}_X$  (NO+NO<sub>2</sub>) is under investigation in this study, the conversion of NO to  $\mathrm{NO}_2$  can be ignored here. For most data processing methods, the measured  $\mathrm{CO}_2$  and pollutant X must be BG corrected (see Section 2.5), as ambient air is mixed into the plume, which also contains  $\mathrm{CO}_2$  and X.

Below is a brief introduction to the different data processing methods used. A summary of the data analysis methods is given in Table 3. We developed a simple live data processing method (*RolMin*) and compare it with the other processing methods as well as with reference on-board measurements.

**Table 3**Overview of the Plume Chasing data processing methods investigated in this study.

Abbreviation	Description
Regression methods	
LinReg	Linear Regression
RobReg	Robust Regression
RolReg	Rolling Regression
BG-correction methods	
BGinterval	BG from BG interval
RolMin	BG from CO <sub>2</sub> backwards
RolMinSym	BG from CO <sub>2</sub> symmetric
RolMinInd	BG from CO2 and pollutant individual
BGinlet	BG from BG inlet

#### 2.4. Regression methods

#### 2.4.1. Linear regression (LinReg)

One of the standard methods to calculate the emission ratios for Plume Chasing is linear regression (LinReg) (Kolb et al., 2004; Canagaratna et al., 2004; Shorter et al., 2005; Herndon et al., 2005; Zavala et al., 2006; Saari et al., 2016; Vojtisek-Lom et al., 2020a). The data for the pollutant X are plotted against  $CO_2$ . The slope of the linear regression line gives the emission ratio  $R_E$ , see Eq. (2).

$$R_E = \frac{\delta[X(t)]}{\delta[CO_2(t)]}$$
 (2)

For all regression methods, the time series of  $CO_2$  ( $[CO_2(t)]$ ) and of the pollutant ([X(t)]) have to be carefully time-aligned with each other. Further, it is assumed that the ratio of pollutant to  $CO_2$  is always the same. This can be critical as the vehicle may exhibit a variable correlation between fuel consumption and emissions of pollutant X. In particular, the emission reduction system can have a variable cleaning efficiency for the pollutant X, as is the case for SCR. Another important aspect is that in a linear regression a single outlier (e.g. from other emission sources) can have a significant influence on the results (Olin et al., 2023).

#### 2.4.2. Robust regression (RobReg)

The application of Robust Regression techniques can reduce the influence of outliers (Wang et al., 2020; Olin et al., 2023; Leinonen et al., 2023). In this study we use the Huber robust regression method (RobReg) (HuberT from python package statsmodels with the tuning constant at the default value of 1.345). The Huber robust regression uses instead of the mean square error loss (linear regression), the Huber loss function, which gives lower weight to outliers. We also tested other robust regression methods (e.g. rstudh, with same parameters for studentized residual and vector of leverage values for the least-square fit like in Wang et al., 2020), which showed no significant differences to the Huber robust regression. As with the LinReg method, it has to be assumed that the ratio of pollutant to  $CO_2$  is constant over time.

For linear and robust regression, the average background of each individual chase is equal to the intercept with the x- and y-axis of the regression line. In some studies the intercept is fixed and set to BG values determined separately from BG intervals before or after each chase (Canagaratna et al., 2004).

#### 2.4.3. Rolling regression (RolReg)

This method uses the 'plume dilution' rolling regression approach (RolReg) introduced by Farren et al. (2023). The method was developed as a single method for different remote sensing techniques, such as Point Sampling or Plume Chasing. As for the other regression methods, no BG subtraction is needed. The pollutant to  $CO_2$  ratio is determined from the slope of the regression lines of always three consecutive measurement points (1 s time resolution). The different slopes obtained from one chase are filtered according to the following criteria: high  $R^2$  values (> 0.95), a slope filter ( $R_E$  > -0.1) and  $\delta[CO_2(t)]$  > 5 ppm.

It has been shown that this technique is perfectly suitable for highemitter identification and the results were found to correlate well with on-board reference measurements (Farren et al., 2023). The advantage of the short duration rolling regression method compared to the other regression approaches is that it can account for changes in the ratio of pollutant to CO<sub>2</sub> throughout a plume chase. Unlike the other methods investigated, the average emission ratios determined for each session are not expected to match the average emission ratios of the SEMS reference data perfectly, as the rolling regression approach uses only a subset of the chasing data where the CO<sub>2</sub> signal changes sufficiently.

#### 2.5. Methods with background (BG)-corrected time series

Another way to determine the emission ratio  $R_E$  is to calculate the averages of the BG-corrected time series of pollutant and  $CO_2$  individually (Hansen and Rosen, 1990), see Eq. (3).

$$R_{E} = \frac{\sum_{t=0}^{T} ([X(t)] - [X_{BG}(t)])}{\sum_{t=0}^{T} ([CO_{2}(t)] - [CO_{2}BG(t)])}$$
(3)

The BG-corrected time series of pollutant and  $\mathrm{CO}_2$  are first averaged before calculating the ratio of pollutant to  $\mathrm{CO}_2$ . This is done to make the measurement more representative of the full driving cycle, similar to PEMS measurements. If the emission ratio were calculated on a second-to-second basis, weak and strong emission periods would be considered equally, even if the weak emission events are less relevant for the total emission. Furthermore, by averaging the time series first, the result is more robust to small inaccuracies in time synchronisation between instruments or differences in response functions. The BG-corrected time series can be calculated using different methods.

#### 2.5.1. BG from BG interval (BGinterval)

A BG interval before and/or after the chase can be used to determine the BG (BGinterval) (Wang et al., 2011, 2012; Ning et al., 2012; Ježek et al., 2015; Lau et al., 2015; Wang et al., 2020; Tong et al., 2022; Xiang et al., 2023; Leinonen et al., 2023). This approach is also called baseline approach. Different measures are used, such as the median (Wang et al., 2020; Leinonen et al., 2023) or the mean (Tong et al., 2022; Ježek et al., 2015) of the emission concentrations of the BG interval. In some cases, high impact data is removed from BG interval data (Wang et al., 2020). The length of the time interval for the calculation of the BG can vary from a few seconds to several minutes. Some approaches determine the BG before and after the chase and average the determined BG values to account for changes during the chase of the vehicle (Wang et al., 2020; Ježek et al., 2015).

As the BG was very stable throughout the day in our study, we chose only a few BG intervals during the day (varying from 15 s to 8 min) to determine the average BG values, see Eq. (4).

$$\begin{aligned} [\mathbf{X}_{\mathrm{BG}}(t)] &= \overline{[\mathbf{X}(t')]}|_{t' \in t_{\mathrm{BG interval}}} \\ [\mathbf{CO}_{2\,\mathrm{BG}}(t)] &= \overline{[\mathbf{CO}_{2}(t')]}|_{t' \in t_{\mathrm{BG interval}}} \end{aligned}$$

This method often requires a lot of manual work and individual postprocessing to ensure that the selected intervals really do not contain any other significant plumes, especially in heavy traffic situations. Also, the frequency of chases is more limited with this method when the background changes a lot, as one needs to make sure that there is a sufficiently long interval between each chase to take a BG measurement.

#### 2.5.2. Rolling minimum

Another method is the rolling minimum approach (Wen et al., 2019; Pöhler et al., 2020; Kelp et al., 2020; Xiang et al., 2023). The BG values are determined as the rolling minimum or 5th percentile values of the time series of the measured signals within a specified time interval (a few minutes) symmetrically around each data point or backwards in time. To reduce the influence of noise in the derived BG value, the

measurement data may be smoothed with a moving average before applying the algorithm to search for the BG value.

We applied a slightly modified version of this method and determined the BG values from the rolling minimum of only  $\mathrm{CO}_2$ . The BG for the pollutant is then defined as the pollutant value at the time of the assigned  $\mathrm{CO}_2$  BG. One advantage of this approach is that the derived minimum for the pollutant X is less influenced by other emission sources, and avoids underestimated BG value of pollutant X. Another advantage is that even if the derived  $\mathrm{CO}_2$  BG value contains some proportion of the emission plume, the proportion in the associated pollutant BG values will be the same and cancelled out in the calculation. It only assumes that the components of the plume are evenly distributed as well as that the pollutant and  $\mathrm{CO}_2$  are emitted at the same time, so that a minimum of  $\mathrm{CO}_2$  emissions would be accompanied by a minimum of pollutant X emissions. For a mathematical proof see Appendix D.

We compare three slightly different methods of processing data using the rolling minimum approach. They are described below. The BG is for all three methods determined from the  $5\,\mathrm{s}$  moving average of the time series of the measured signals.

#### BG from CO<sub>2</sub> backwards (RolMin)

Here the minimum  $\mathrm{CO}_2$  value within a specified time interval (120 s) prior to each data point is designated as the background value (*RolMin*). The BG for the pollutant is defined as the pollutant value at the time of the assigned  $\mathrm{CO}_2$  BG, see Eq. (5).

$$\begin{aligned} [X_{BG}(t)] &= [X(\underset{t' \in [t-120,t]}{arg \min} [CO_2(t')])] \\ [CO_{2BG}(t)] &= \underset{t' \in [t-120,t]}{\min} [CO_2(t')] \end{aligned}$$
 (5)

The optimum length of the time interval depends on the road profile, especially the gradient, and the length of chases. If the BG changes a lot, e.g. due to different influences from the surrounding or different road profiles, a shorter BG interval is appropriate. If the BG is relatively stable and the road conditions are such that constantly high emission concentrations are measured from the plume (vehicles under constant load), a longer time interval is recommended.

#### BG from CO<sub>2</sub> symmetric (RolMinSym)

To check the robustness of the *RolMin* approach, we investigate whether the chosen time interval has a significant influence. Therefore, in the second rolling minimum approach the  $CO_2$  value is determined from a time window symmetrically  $\pm 60\,\mathrm{s}$  around each individual measuring point (*RolMinSym*) (see Eq. (6)).

$$\begin{aligned} [X_{BG}(t)] & = [X(\underset{t' \in [t-60,t+60]}{arg \, min} [CO_2(t')])] \\ [CO_{2BG}(t)] & = \underset{t' \in [t-60,t+60]}{min} [CO_2(t')] \end{aligned}$$
 (6)

#### BG from CO<sub>2</sub> and pollutant individual (RolMinInd)

The third rolling minimum approach is in line with most of the algorithms described in the literature and determines the BG of  $\rm CO_2$  and the pollutant individually (*RolMinInd*). The BG values are defined as the lowest values within a particular time interval of 120 s before each individual point of measurement (see Eq. (7)).

$$[X_{BG}(t)] = \min_{t' \in [t-120,t]} [X(t')]$$

$$[CO_{2BG}(t)] = \min_{t' \in [t-120,t]} [CO_{2}(t')]$$
(7)

This method can have advantages when determining the emissions of PM, as discussed in Section 3.2.6, but may also have significant drawbacks due to the influence of other emission sources or variable background, resulting in overestimated emission values (see Section 3.2.6).

#### 2.5.3. BG from BG inlet (BGinlet)

In this study we also measured the BG with an additional inlet on the roof of the chasing vehicle (BGinlet) (see Eq. (8)).

$$[X_{BG}(t)] = [X_{BG inlet}(t)]$$

$$[CO_{2BG}(t)] = [CO_{2 BG inlet}(t)]$$
(8)

The location of the additional inlet on the roof of the vehicle was optimised in previous studies of the CARES project to measure as little of the plume signal as possible. For this method, the BG data time series must be carefully time-aligned and offset-corrected to be in line with the plume signal data set. An offset would lead to emission ratios that are systematically too high or too low. With the other methods, the offset-correction was irrelevant, as the BG was determined from the plume signal time series, so that only a difference signal was formed, in which offsets play no role.

#### 2.6. Measurements on-board the investigated vehicles

#### 2.6.1. NO<sub>x</sub> with SEMS

In this study, the average  $NO_x/CO_2$  ratios of three of the test vehicles (two LDVs and one HDV), determined by different Plume Chasing data processing methods, are compared with reference  $NO_x/CO_2$  ratios from on-board SEMS measurements (Spreen et al., 2016). The SEMS data was time-synchronised with the Plume Chasing data. For the calculation of the SEMS  $NO_x/CO_2$  ratios  $R_E$ , the mass flows of  $NO_x$  and  $CO_2$  are averaged over the chasing time period (see Eq. (9) with  $[X_{ref}(t)] = [NO_x_{SEMS}(t)]$  and  $[CO_{2ref}(t)] = [CO_{2SEMS}(t)]$ ). Only  $CO_2$  and  $NO_x$  values with an associated  $CO_2$  level above 1 %  $CO_2$  mixing ratio are included in the average ( $[CO_{2SEMS}(t)] > 1$ %), as periods with lower emissions are on average less relevant for the total emissions, but have higher relative error. Furthermore, in situations with low emissions there is no detectable plume with Plume Chasing. The 'on-board' emission ratio was then determined as:

$$R_E = \frac{\sum_{t=0}^{T} [X_{\text{ref}}(t)]}{\sum_{t=0}^{T} [CO_{2\text{ref}}(t)]}$$
(9)

 $[{\rm NO_{x\,SEMS}(t)}]$  is measured with a low-cost  ${\rm NO_{x}}$  sensor, whereas  $[{\rm CO_{2\,SEMS}(t)}]$  is calculated from on-board diagnostics (OBD) readings (Spreen et al., 2016). Deviations between SEMS and the established PEMS can reach several percent as the SEMS uses a ZrO\_2-based sensor, which has a NO\_x measurement tolerance of  $\pm 20\,\rm ppm$  below 100 ppm (Yu et al., 2021). The median NO\_x values measured by SEMS were 118 ppm for the HDV, 27 ppm for the VW Caddy and 72 ppm for the VW Transporter.

#### 2.6.2. NO measurements with Mini-PEMS

The NO and  $\mathrm{CO}_2$  emissions of the motorcycle and scooter were measured by a Mini-PEMS, a highly compact,  $10\,\mathrm{kg}$ ,  $40\times20\times20\,\mathrm{cm}$  portable on-board emission monitoring system developed and validated for on-road motorcycle measurements (Vojtisek-Lom et al., 2020b). The instrument was built by the Technical University of Liberec, Czech Republic. The system uses an NDIR analyser for HC, CO,  $\mathrm{CO}_2$  and electrochemical cells for NO,  $\mathrm{NO}_2$  and  $\mathrm{O}_2$  measurements and employs the speed-density method for estimation of the exhaust flow. The Mini-PEMS were installed on the luggage rack of the motorcycles (Fig. B.14). The emission ratios were then calculated according to Eq. (9) (with  $[\mathrm{X}_{\mathrm{ref}}(t)] = [\mathrm{NO}_{\mathrm{Mini-PEMS}}(t)]$ ,  $[\mathrm{CO}_{\mathrm{2\,ref}}(t)] = [\mathrm{CO}_{\mathrm{2\,Mini-PEMS}}(t)]$  and  $[\mathrm{CO}_{\mathrm{2\,Mini-PEMS}}(t)] > 1\,\%$ ).

#### 2.6.3. PN with TEN AEM and NanoMet3

On-board the VW Caddy,  $PN_{23}$  measurements were performed with the TEN AEM and  $PN_{10}$  measurements with a NanoMet3 instrument (measurement range:  $1\times10^4-3\times10^8$  #/cm³; 10-700 nm). Both instruments measure solid (non-volatile) PN. The  $CO_2$  data used to calculate the emission ratios was available from the SEMS data. The emission ratios were then calculated according to Eq. (9) (with  $[X_{ref}(t)] = [PN_{10}(t)]$  or  $[PN_{23}(t)]$ ,  $[CO_{2\,ref}(t)] = [CO_{2\,SEMS}(t)]$  for all data with  $[CO_{2\,SEMS}(t)] > 1$ %).

#### 2.7. Data filters

Plume Chasing measurements were only considered valid if the  $\mathrm{CO}_2$  mixing ratio exceeded the BG by more than  $20\,\mathrm{ppm}$  ([ $\mathrm{CO}_2(t)$ ] – [ $\mathrm{CO}_{2\,\mathrm{BG}}(t)$ ] >  $20\,\mathrm{ppm}$ ) to ensure that only sufficiently strong plume signals were considered. A threshold of  $20\,\mathrm{ppm}$  was considered reasonable in this case since the BG was very stable on the test track. For the evaluation of the emissions of the motorcycle and scooter, a threshold value of 5 ppm was used. This was necessary because only a small plume is measured for these vehicles, especially during high speed sessions (larger distance to the chased vehicles). The scooter and motorcycle were always driving either in front of the other vehicles or with a large distance to the other vehicles (non-convoy driving), so there was no interference from other vehicles and such a low threshold could be applied. For measurements in areas with heavy traffic (highways) and other emission sources, a higher threshold of 30 ppm is recommended.

In addition, two speed filters were used to reduce the influence of plumes from other vehicles. Measurements were only considered valid when the Plume Chasing vehicle speed was greater than 10 km/h, as at higher speeds the vehicle aerodynamics tend to keep the emissions in the vehicle wake, whereas at lower speeds the emissions can spread more to the side or ahead. In this case it is then not clear which plume is being measured; it may even be the plume from the chasing vehicle itself. Furthermore, measurements were only considered valid if the wind speed in the driving direction (measured at the roof of the vehicle) was less than the vehicle speed (to ensure that the vehicle's own plume was not measured). In addition, a filter was applied so that only those times when SEMS data were available were included in the calculation of the Plume Chasing data.

#### 3. Results and discussion

#### 3.1. Overview of measured vehicle emissions

Table 4 provides an overview of the  $\mathrm{NO_x}$ , NO and  $\mathrm{PN_{10}}$  emissions of the tested vehicles measured by on-board SEMS, Mini-PEMS and NanoMet3 respectively (see also Fig. 9, left). A distinction is made between tampered and non-tampered exhaust aftertreatment system state (SCR, DPF).

The average  $NO_x/CO_2$  emission ratios for the HDV Ford Truck ranged from 0.9 (non-tampered) to 76.8 ppm/% (tampered). This corresponds to energy-specific emission factors of 63 and 5345 mg/kWh, assuming an engine efficiency of 40%. For the LDVs (VW Caddy and VW Transporter), the emission ratios ranged from 2.3 (non-tampered) to 21.3 ppm/% (tampered). This corresponds to distance-based emission factors of about 37 and 276 mg/km with a type-approval  $CO_2$  of 124 and 155 g/km for the VW Caddy and VW Transporter, respectively. Median emission ratios are close to the average values and between convoy and non-convoy driving there were only minor differences in the measured reference values (see Table C.7 in the Appendix).

The  $NO_x/CO_2$  emission ratios measured by Plume Chasing (*RolMin*) are shown in Fig. C.15 and in Table C.7 in Appendix A. The emission ratios are close to the reference values for the Ford truck, VW Caddy and VW Transporter. The median  $NO_x$  emissions of the motorcycle and scooter calculated from the Plume Chasing measurements were between 0.6–2.1 ppm/%. This corresponds to approximately 56–110 mg/km, assuming 98 g/km  $CO_2$  for the motorcycle and 52 g/km for the scooter. The median PN emissions of all vehicles measured by Plume Chasing (Fig. C.16) were relatively low ranging between approximately 5–207  $\cdot 10^{10}$  #/kg<sub>fuel</sub> for PN<sub>@90</sub>, 6–29  $\cdot 10^{13}$  #/kg<sub>fuel</sub> for PN<sub>23</sub> and 7–49  $\cdot 10^{13}$  #/kg<sub>fuel</sub> for PN<sub>2.5</sub>. Lower emissions were measured for the diesel vehicles with DPF (Ford truck, VW Caddy, VW Transporter) and higher emissions for the gasoline vehicles (motorcycle, scooter, VW Touran).

Table 4
Mean  $NO_x/CO_2$  emission ratios from on-board SEMS measurements for the Ford truck, VW Caddy, and VW Transporter; mean  $NO/CO_2$  ratios from Mini-PEMS measurements for the Motorcycle and Scooter; and  $PN_{10}/CO_2$  ratios from NanoMet3 measurements for the VW Caddy. Sessions in which the tampering status was just changed, as well as cold SCR situations, are excluded from the  $NO_x$  data.

	$NO_x/CO_2$ [ppm/%]			NO/CO <sub>2</sub> [ppm	1/%]	$PN_{10}/CO_2$ [#/kg <sub>fuel</sub> ] · 10 <sup>13</sup>	
	Ford truck	VW Caddy	VW Transporter	Motorcycle	Scooter	VW Caddy	
Tampered	$76.8 \pm 20.3$	$21.3 \pm 9.5$	$18.2 \pm 4.6$			4.4 ± 1.7	
Non-tampered	$0.9 \pm 0.8$	$4.4 \pm 3.1$	$2.3 \pm 2.1$	$0.3 \pm 0.5$	$2.4 \pm 2.0$	$1.2 \pm 0.1$	

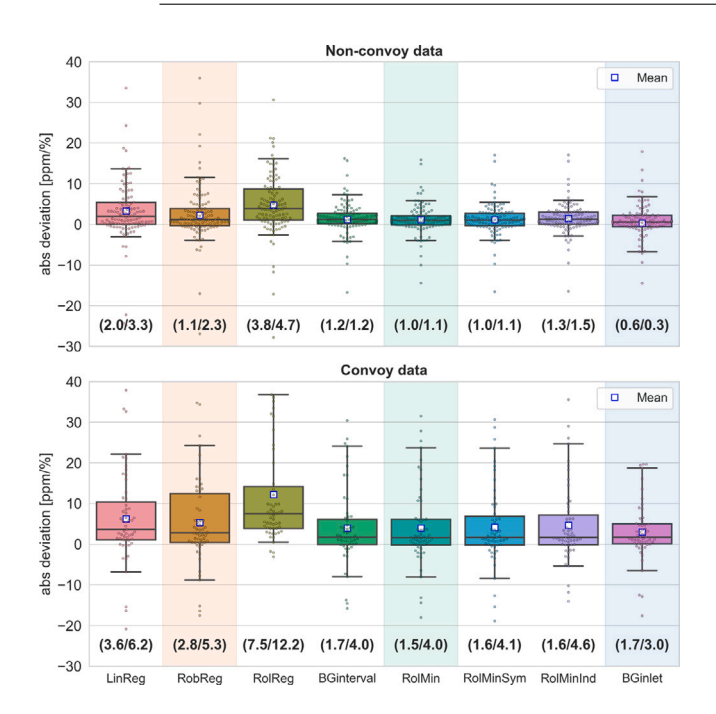


**Fig. 3.** Comparison of different Plume Chasing data processing methods for  $NO_x/CO_2$  ratios. Compared are the absolute deviation to SEMS ratios. Top: non-convoy driving, bottom: convoy driving. The median/mean absolute deviation of each method is given in brackets below each box-plot. The whiskers represent the 5th and the 95th percentiles. One individual data point is the result of (usually) one lap for one vehicle. The median/mean SEMS  $NO_x/CO_2$  ratios are 9/19 and 7/17 ppm/% for non-convoy and convoy data respectively.

#### 3.2. Comparison of plume chasing data processing methods

#### 3.2.1. Comparison to reference SEMS data

The average NO<sub>x</sub>/CO<sub>2</sub> emissions per chase and vehicle are calculated from the Plume Chasing data using the different data processing methods presented in Sections 2.4 and 2.5 and compared to the average SEMS NO<sub>x</sub>/CO<sub>2</sub> emission ratio derived according to Section 2.6. The absolute deviations for all vehicles are shown separately for convoy and non-convoy driving (Fig. 3). The average emissions determined by Plume Chasing show higher values compared to the average SEMS emission values for all investigated methods, but agree within the errors of the SEMS. In the non-convoy sessions, the emissions deviate only slightly from the SEMS values. In the convoy sessions, however, the deviation is more pronounced. While the different BG correction methods do not differ significantly from each other, the three different regression methods show higher absolute deviations from the SEMS values: The 95th percentile for non-convoy driving is for the different BG correction and regression methods  $\sim 8 \text{ ppm}/\%$  and  $\sim 14-20 \text{ ppm}/\%$ , respectively. For convoy driving this increases to ~ 22 ppm/% and  $\sim 21-38 \, \mathrm{ppm}/\%$  respectively. The deviation (overestimation) of the RolMinInd method is slightly higher compared to the other rolling minimum methods. This is expected (see Section 2.5.2), as the BG-corrected time series of the pollutant is strictly higher or equal compared to the BG-corrected time series of the RolMin or RolMinSym method. The BGinterval method gives very similar results to the rolling minimum

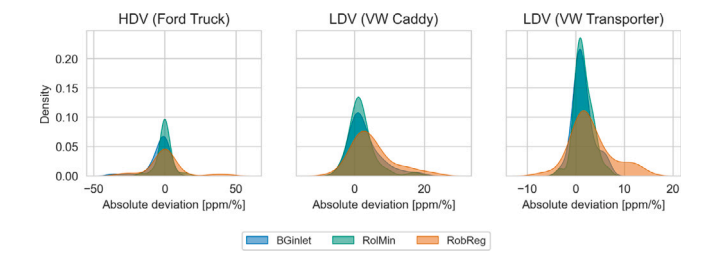


Fig. 4. Distributions of the absolute deviations of  $NO_\chi/CO_2$  Plume Chasing to SEMS emission ratios of the methods *BGinlet* (blue), *RolMin* (green) and *RobReg* (orange) for the Ford truck (left), VW Caddy (middle) and VW Transporter (right). Only non-convoy data is included. (For interpretation of the references to colour in this figure legend, the reader is referred to the web version of this article.)

methods for both, convoy and non-convoy driving. This emphasises the ability of the rolling minimum approaches to determine similar BG values to the *BGinterval* method, with the advantage that they can be easily automated and that no additional time is required to measure the BG without interference as for the *BGinterval* method. The *BGinlet* method shows the smallest mean (and median for non-convoy) absolute deviation. For non-convoy driving this is mainly due to the fact that the method underestimates the emissions to a greater extent than other methods (the 5% percentile is at  $\sim$  -8 ppm/%). For convoy driving the underestimation is similar to other methods, but the overestimation is less pronounced (5% percentile is with  $\sim$  19 ppm/% the lowest).

To see whether there are any differences in the absolute deviations between the three vehicles studied, their individual density distributions (only non-convoy) are shown in Fig. 4. Three of the evaluated methods, RobReg shaded in orange, RolMin shaded in green and the method with the BG measurement on the roof of the chasing vehicle (BGinlet) shaded in blue, are shown. The two LDVs show a right-skewed density distribution, whereas the HDV shows a more symmetrical density distribution. This means that in this constellation the emissions of the LDVs tend to be estimated higher by the different Plume Chasing data processing methods than by the on-board SEMS measurements. This could also result from higher SEMS uncertainties for lower emission values (Section 2.6), as the vehicle with the lowest emissions values (VW Caddy) has the strongest right-skewed distribution (see also discussion in Section 3.2.5). In case of convoy data (Fig. F.21 in the Appendix) the density distribution gets broader (higher deviations from the reference SEMS values) and more strongly right-skewed for the LDVs, in case of the HDV it appears more strongly left-skewed. This can be explained by the fact that the LDVs used had a lower average emission ratio than the HDV for both the non-tampered and the tampered data combined. The vehicles with the lower emission ratio are interfered by the vehicle with the higher emission ratio, resulting in an overestimation and vice versa. Further results of all investigated methods for each vehicle separately can be found in the Appendix (Figs. F.22-F.24).

#### 3.2.2. Influence of speed filter, smoothing and the CO<sub>2</sub> sensor

As mentioned in Section 2.7, the application of a speed filter can improve the accuracy of the emission ratios determined from the measurements. The set minimum speed level depends mainly on the wind conditions and the type of nearby/chasing vehicle. In this study

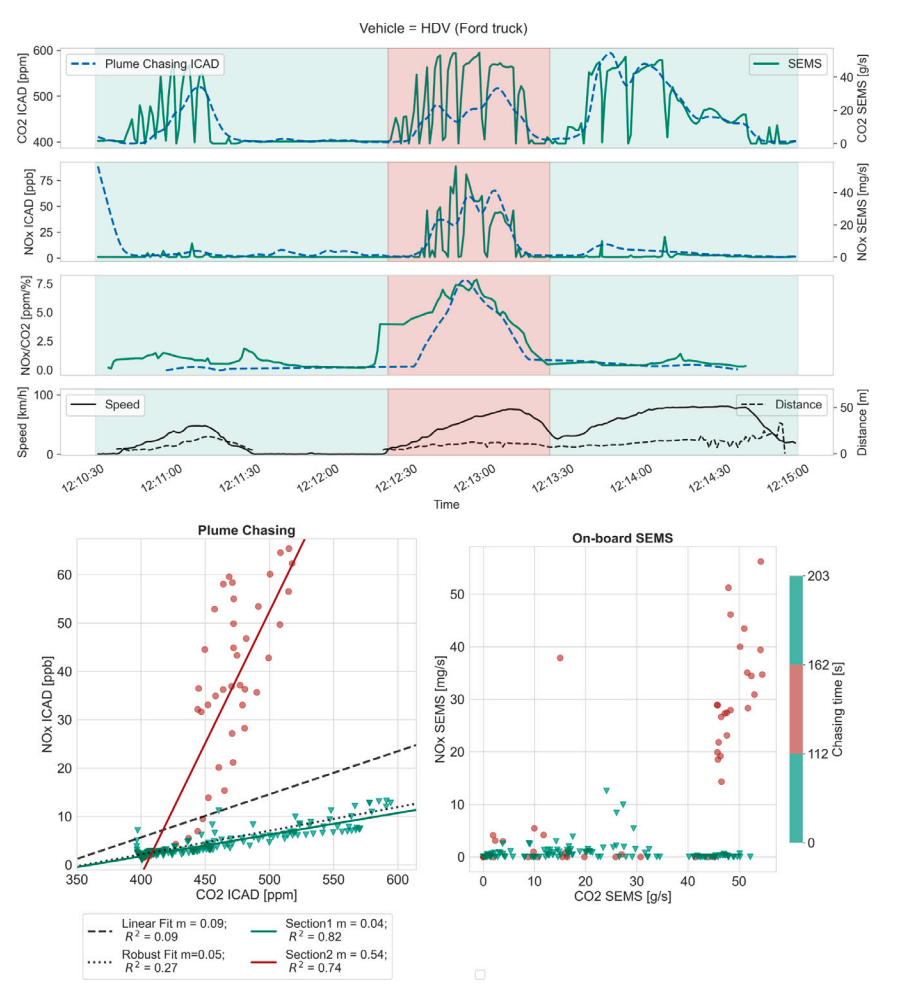


Fig. 5.  $CO_2$  and  $NO_x$  time series for the HDV, measured by Plume Chasing (blue) and SEMS (green) for one lap of the test track (upper panel). The red shaded area represents when HDV  $NO_x$  emissions were higher than the rest of the lap (green shaded areas).  $NO_x$  vs  $CO_2$  scatter plots for the Plume Chasing and SEMS (lower left and right panel respectively). The colour of the data points corresponds to the section of the chase time in the time series shown above. Regression lines of the *LinReg* (dashed black line) and *RobReg* (dotted black line) methods are shown. (For interpretation of the references to colour in this figure legend, the reader is referred to the web version of this article.)

we found the best setting to be  $v>10\,\mathrm{km/h}$ . Smoothing the data, i.e. reducing the time resolution, did not improve the results in our case, probably because the data was already sufficiently aligned between different instruments and the choice of instruments was optimised. Investigations into the use of a medium-cost  $\mathrm{CO}_2$  sensor vs. high grade instruments for Plume Chasing found only negligible differences in calculated emission factors. A more detailed analysis of these parameters can be found in Appendix G.

#### 3.2.3. Constrains of linear and robust regression

Although the *LinReg* and *RobReg* methods have the advantage that no BG has to be explicitly determined (see Section 2.4), the average emissions determined by the *LinReg* and *RobReg* methods deviate more from the SEMS reference values compared to the methods where the BG has to be determined (Fig. 3). The assumption for these methods is that the ratio of pollutant to  $\rm CO_2$  is constant at all times (Section 2.4.1). An example where this is not the case is illustrated in Fig. 5 for one chase of the HDV. The ratio of  $\rm NO_x$  to  $\rm CO_2$  changes when different subsets of data are processed. The HDV emissions are higher for a short time in between (red shaded area and red data points). While the *RolMin* method gives an emission ratio  $(1.4\,\rm ppm/\%)$  with the smallest deviation of  $30\,\%$  to the SEMS emission ratio  $(2.0\,\rm ppm/\%)$ , the *LinReg* method underestimates the emissions by about  $50\,\%$  ( $0.9\,\rm ppm/\%$ ). The robust regression, which reduces the weights of the high impact points (high emission

points), underestimates the emissions by  $\sim 75\,\%$  (0.5 ppm/%). Such high impact points which are largely ignored by the robust regression method, can come from e.g. a variable cleaning efficiency of emission reduction systems or from engine motoring events (Karjalainen et al., 2016) or external sources. If they come from external sources, the *RobReg* method helps to improve the results by reducing the influence of individual outliers. This is discussed in detail in Olin et al. (2023). However, if the short events are caused by the engine or SCR system of the chased vehicle, they are also ignored and are not included in the calculated emissions, even though they are part of the relevant vehicle emissions. Fig. H.26 in the Appendix shows an example where all three methods work similarly well and where the determined emission ratios are close to the SEMS emission ratios (1–4 % deviation).

#### 3.2.4. Robustness of the Rolling Minimum (RolMin) method

To investigate the robustness of the *RolMin* results with varying time intervals for automatic BG determination, we assessed the influence of firstly a symmetrically  $(\pm 60 \, \text{s})$  determined BG (see Section 2.3, *RolMinSym* method) and secondly different lengths of time intervals  $(t=60 \, \text{s}, 120 \, \text{s}, 240 \, \text{s} \text{ and } 480 \, \text{s})$  on the *RolMin* method.

In the case of a symmetrically determined BG (*RolMinSym*) the change in average emissions for the LDVs and the truck is very small with around  $\pm 1\,\%$ . The change for the two 2-wheeled vehicles is higher (-6–10%), likely due to the weak measurement signal compared to

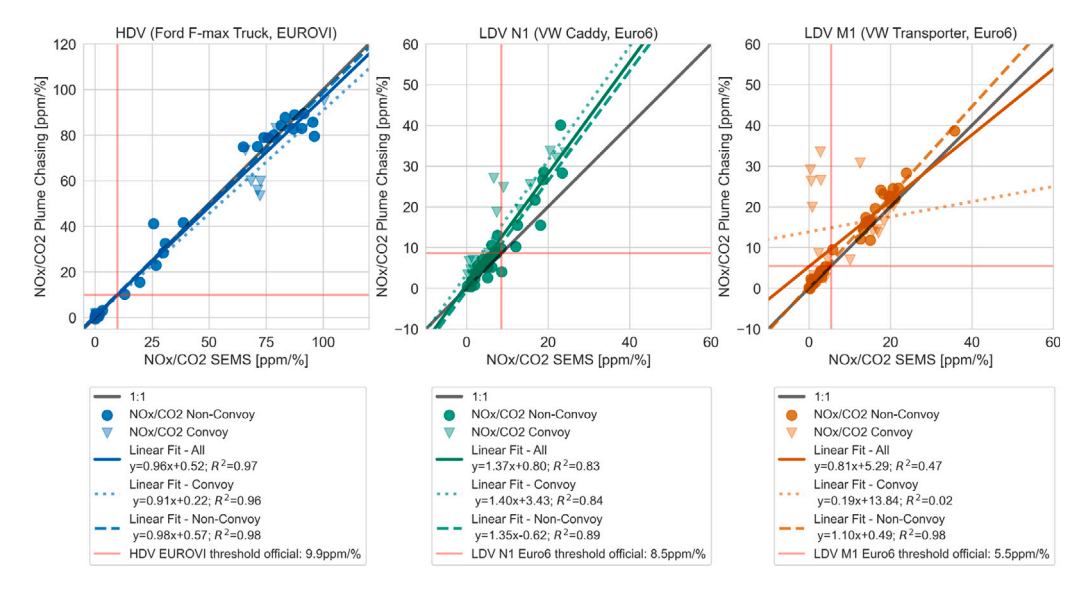


Fig. 6. Scatter plot  $NO_x/CO_2$  Plume Chasing (RollMin) vs. SEMS of Ford truck (left), VW Caddy (middle) and VW Transporter (right). Each data point is the derived emission value of one driving constellation (typically one lap - 2.8 km), for convoy driving (triangles) and non-convoy driving (circles). The official Euro 6 threshold for the HDV and the LDVs are shown as red lines. The data includes both tampered and non-tampered measurements. (For interpretation of the references to colour in this figure legend, the reader is referred to the web version of this article.)

the background fluctuation. Not only the mean and median values of the *RolMinSym* for the different vehicles agree well with the *RolMin* method, but also individual measurements (Fig. I.28, left, in the Appendix). Only few data points show slightly higher absolute deviation of several ppm/%.

When the length of the BG interval is changed, the observed changes in average emissions for the LDVs and the truck are slightly higher at  $\pm 9\,\%$  and  $\sim \pm 22\,\%$  respectively, with lower emission ratios for longer BG intervals. Fig. 1.28 (right) shows that most of the individual emission ratios are lower for the longer BG interval and that not just a few outliers are responsible for the lower average emission ratios. This could be explained by the greater impact of  $\text{CO}_2$  uncertainties on emission ratios compared to pollutant uncertainties (Wang et al., 2011). If the BG interval is very long (in this study 480 s),  $\text{CO}_2$  will remain at the lowest value for the entire chase, even though fluctuations in the BG lead to higher average  $\text{CO}_2$  BG values.

In general, it was found that changing the time interval (length and position around measurement point) has little effect on the determined average emission ratios per vehicle (Fig. I.27 in the Appendix).

#### 3.2.5. The effect of convoy vs non-convoy driving

A scatter plot of the derived NO<sub>x</sub>/CO<sub>2</sub> ratios measured by Plume Chasing and calculated with the RolMin method against those of SEMS is shown in Fig. 6 for the Ford truck (left), the VW Caddy (middle) and the VW Transporter (right). The Plume Chasing RolMin method shows excellent correlation with the averaged SEMS NO<sub>x</sub> data for nonconvoy driving of all three vehicles. The coefficient of determination is highest for the truck and VW Transporter with  $R^2 = 0.98$  and lowest for the VW Caddy ( $R^2 = 0.89$ ). The NO<sub>x</sub>/CO<sub>2</sub> ratios agree within  $\sim 2\%$  for non-convoy driving between Plume Chasing and SEMS for the truck. For the VW Transporter the agreement is within the range of  $\sim 10\%$ , but for the VW Caddy it is  $\sim 35\%$  significantly lower. Since the Plume Chasing emission results agree well for the truck and the VW Transporter, and the VW Caddy was measured in sessions with the same driving characteristics and with the same Plume Chasing instruments, the deviations between the SEMS and Plume Chasing NO<sub>x</sub>/CO<sub>2</sub> ratios could be due to a systematic underestimation of the NO<sub>x</sub>/CO<sub>2</sub> ratios by the SEMS instrument installed in the VW Caddy. Deviations between SEMS and the PEMS can reach several percent (Yu et al., 2021; Spreen et al., 2016). This is because the SEMS uses a ZrO<sub>2</sub>-based sensor, which has a  $NO_x$  measurement tolerance of  $\pm 20 \, ppm$  below 100 ppm. The VW

Caddy had the lowest median SEMS  ${\rm NO_x}$  values (27 ppm, compared to 118 ppm for the HDV and 72 ppm for the VW Transporter) and with this the highest relative uncertainties for the SEMS measurement. The underestimation could also be specific to the SEMS installed in the VW Caddy or due to some vehicle characteristics. This could be investigated in future campaigns by exchanging the SEMS between vehicles or validating the SEMS with a PEMS. For the following investigations in this study the SEMS emission ratios of the VW Caddy have been corrected by a factor of +35 % unless otherwise stated (it is assumed here that the SEMS is underestimating the true emissions of the VW Caddy).

For convoy driving the correlation is lower for all vehicles ( $R^2$  = 0.96 for the truck,  $R^2 = 0.84$  for the VW Caddy and  $R^2 = 0.02$ for the VW Transporter). The main cause of larger deviations from the reference data was found to be situations where emissions are significantly influenced by other plumes (Fig. 6, triangular data points for convoy measurements), e.g. a passenger car driving closely behind a very high-emitting truck with a deactivated SCR system (Fig. 7). In the case of the VW Transporter, about  $\alpha = 35(5)\%$  of the emission ratio determined by the RolMin method came from the high-emitting truck (Veh1) driving directly in front of the VW Transporter (Veh2) ( $R_{E~PlumeChasing~Veh2} = (1 - \alpha)R_{E~SEMS~Veh2} + \alpha R_{E~SEMS~Veh1}$ ). The weaker LDV plume (in terms of volume) is therefore overlaid by the stronger HDV plume. The emission measurements of the VW Caddy, which was driving in third place behind the high-emitting truck, were only mildly affected ( $\alpha = 6(4)\%$ ). If the truck (non-tampered) was measured with the tampered VW Transporter directly in front, about  $\alpha = 5(2)\%$  of the measured emission signal came from the high-emitting LDV driving directly in front of the HDV. In the case of the tampered VW Caddy driving directly in front of the non-tampered VW Transporter,  $\alpha =$ 22(18)% of the measured emission signal came from the high-emitting LDV. In general, a weak plume (weak CO2 signal) is more likely to be influenced by other emission sources than a strong emission plume. Conversely, a strong HDV plume will not be significantly influenced by a weak LDV plume. Possible ways to reduce the influence of other vehicles on the observed emission value are:

- · Avoid busy roads.
- · Avoid measuring a LDV behind a HDV.
- If there is a vehicle directly in front of the measured vehicle also measure the vehicle in front and reject the measurement if the emission ratio from the vehicle in front is significantly higher.



Fig. 7. Scheme of the main cause of false positive light duty high-emitters. This situation should be avoided or the HDV in front should also be measured.

The other investigated Plume Chasing methods show similar results when comparing convoy and non-convoy driving. The general observations already discussed in Section 3.2.1 can also be observed here. The BGinlet method stands out in this comparison, showing smaller absolute deviations from the average SEMS emission ratios for LDVs in convoy sessions compared to the other methods (-2.5 ppm/% on average for the VW Transporter). The average emission ratios determined by the BGinlet method can be up to 30% lower than for the other methods. With this, the influence of the high-emitting truck driving directly in front of the VW Transporter is reduced by 11 % to  $\alpha = 24(12)$  %. This can be explained by the fact that the BG is measured by an additional inlet on the roof of the vehicle. As a result, the plume from e.g. a high-emitting HDV driving in front of the non-tampered LDV is also partly included in the BG. How well the BG on the roof is representative depends mainly on factors such as the shape of the vehicles in front and the wind conditions. If contamination from other vehicles or sources is not well represented in the BG inlet, the BGinlet method will be less beneficial. In general, however, HDV emissions are slightly lower  $(\sim 5\%)$  for the BGinlet method compared to the other methods, slightly increasing the difference between SEMS and Plume Chasing (Fig. J.29 in the Appendix). This could be due to the fact that the BGinlet method measures not only the BG with the BG inlet, but measures also a significant part of the plume of the measured vehicle directly in front (HDV). As a result, the BG-corrected signal is lower and there are fewer data points above the CO<sub>2</sub> threshold that count towards the emission ratio calculation (15 % fewer data points for the HDV compared to  $\sim 6$  % fewer for the LDVs). This can increase the differences with SEMS data, especially for the HDV.

#### 3.2.6. Plume Chasing analysis method for PN

It can be seen that for gaseous compounds such as NOx, the time at which the measured CO2 concentration has its minimum/maximum coincides very well with the minimum/maximum of the gaseous pollutants (Fig. E.20 in the Appendix). In the case of PN, this is not always the case. Factors contributing to a lower correlation between CO2 and PN data could be the engine or after-treatment system, PN measurement including volatile and semi-volatile particles, or relatively low PN measurements accompanied by interference from other vehicles and sources. If the BG for PN is then defined as the PN value at the time stamp of the assigned CO2 BG, this can lead to an overestimation of the BG value for PN (Fig. E.20 in the Appendix) and negative average PN values will be observed in a significant number of cases. To avoid this, the BG of CO2 and PN is determined individually by using the RolMinInd method. This results in systematically higher emission values, as with the RolMin method (example in Fig. E.20 in the Appendix).

All investigated vehicles had relatively low average emissions of PN (Fig. C.16 in the Appendix). The average  $PN_{@90}$  emissions are between  $5\cdot 10^{10}\,\#/kg_{\rm fuel}$  and  $2.07\cdot 10^{12}\,\#/kg_{\rm fuel}$ , with the highest  $PN_{@90}$  emissions measured for the VW Touran. We use the  $PN_{@90}$  measurements for the discussion because they show the best agreement to differentiate between different tampering states of the VW Caddy (see Section 3.4). Differences between the *RolMinInd* and *RolMin* data processing methods are more pronounced for PN (–36.6% on average) than for  $NO_x$  (–11.7%) and more pronounced for low PN emitters than for higher

Table 5 Overview of the median  $PN_{@90}$  and  $NO_x$  emission ratios of investigated vehicles by methods *RolMinInd* and *RolMin*. Median values are determined for each vehicle individually.

Vehicle	PN <sub>@90</sub> [#/I	$(g_{fuel}] \cdot 10^{10}$	NO <sub>x</sub> [ppm,	$NO_x$ [ppm/%]		
	RolMin	RolMinInd	RolMin	RolMinInd		
Ford truck	1.7	5.1	30.4	31.6		
VW Caddy	29.8	36.3	6.7	6.8		
VW Transporter	9.9	14.2	14.2	14.4		
VW Touran	199	207	8.9	9.0		
Motorcycle	-6.1	21.4	0.6	1.0		
Scooter	5.7	26.0	2.1	2.7		

emitters (e.g.  $-67\,\%$  for the HDV and  $3.9\,\%$  for the VW Touran) (see Table 5 and Fig. K.30 in the Appendix). Particularly for the very low PN emitters in the study, the RolMin method shows many negative average emission ratios (approximately 30% for the HDV, 10% for the VW Transporter or 60% for the motorcycle). The lower the measured emissions, the greater the influence of non-exhaust emissions, re-suspension or emissions from other vehicles. Also, it can be observed that vehicles with tampered SCR systems show a higher rate of negative PN values. One reason could be that SCR dosing affects PN emissions, although emissions should generally be higher, as shown by Mamakos et al. (2019). Determining the BG of the pollutant individually from the time series results in fewer negative emission ratios (about 0 % for all vehicles). The extent of this overestimation also depends on the level of emissions from other sources, or the influence of the volatile particle fraction, particularly as they are not a conserved quantity. The particle metrics (e.g. PN, BC), their characteristics (e.g. size range, including/excluding volatiles) and the instrumentation used have a significant influence on whether there can be a large influence from other sources on the results. PN is a general metric that can include various sources, unlike BC, which is specific to combustion emissions. The TEN (PN23) instrument measures non-volatile particles in the size range from 23 nm to several hundred nm, which already limits the size range to the accumulation (soot) mode particles typical of combustion engine processes. The SMPS (PN@90) with the 90 nm setting only measures particles around 90 nm, which specifically filters out if a diesel accumulation mode is present (Fiebig et al., 2014). In the case of test track measurements, environmental influences should be low, as the validation experiments were carried out on an isolated test track. The influence is limited to the non-exhaust emissions and the emissions of the other vehicles on the test track. The measurement of solid PN (excluding volatiles) should be preferred in the future, especially for high emitter identification, as the results are more reproducible.

#### 3.3. Real traffic measurements

The average  $NO_x/CO_2$  emission ratios of the real traffic Plume Chasing measurements are shown in Fig. 8 on the left. On-board SEMS measurements are shown in orange. Plume Chasing shows higher average  $NO_x$  emissions compared to the SEMS emissions ( $\sim 150$ – $300\,\%$ ). The deviations are more pronounced than for the test track results for the VW Caddy ( $\sim 40\,\%$ ). It should be noted that the  $NO_x$  emissions of the VW Caddy are very low. Therefore, a high percentage deviation from

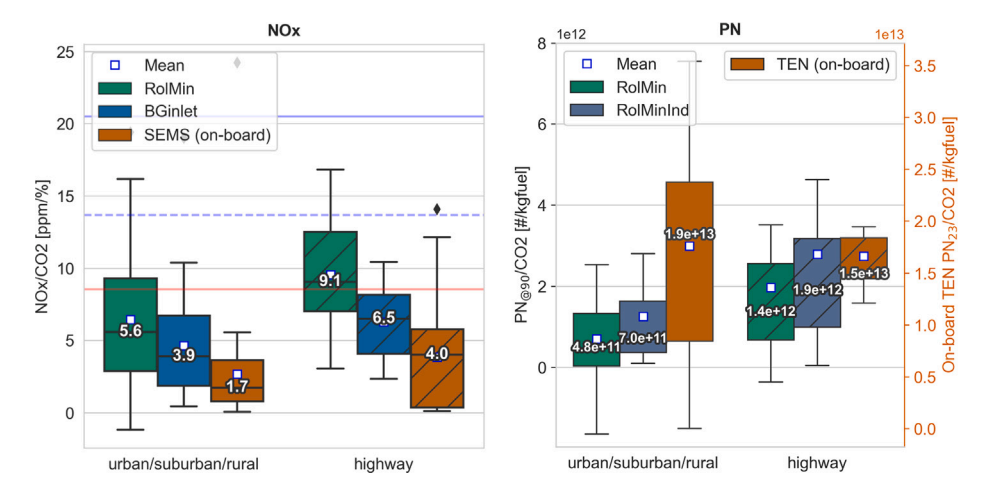


Fig. 8. Average  $NO_x/CO_2$  (left) and average  $PN_{@90}/CO_2$  and  $PN_{23}/CO_2$  (right) for urban/suburban/rural and highway sections. The average Plume Chasing emission results of different methods are displayed (green, blue) as well as average on-board measurements (orange). The Euro 6 N1 emission standard (red line) as well as the suspicious (blue dashed line) and high-emitter (blue solid line)  $NO_x$  thresholds for Euro 6 vehicles (see Section 3.4) are also displayed. The average SEMS  $NO_x/CO_2$  values are corrected by a factor of 35% (see Section 3.2.5). The whiskers represent the 1.5 interquartile range (IQR). (For interpretation of the references to colour in this figure legend, the reader is referred to the web version of this article.)

the reference is still only a small deviation in absolute terms. The higher Plume Chasing results are still close to the Euro 6 emission standard of the VW Caddy (8.5 ppm/%). The low emissions of the VW Caddy compared to the general fleet on the road result in a higher interference from other vehicles. An average of 18 ppm/% was determined for the fleet from Plume Chasing measurements (76 HDVs and LDVs) on 17th and 18th June 2021. This is in line with other studies of vehicle emissions in the Netherlands (van Eijk et al., 2024; Ligterink, 2024) and more than ten times the average SEMS  $\rm NO_x$  emissions of the VW Caddy. The *BGinlet* method gives about 30 % lower  $\rm NO_x$  emissions compared to the *RolMin* method for both measurement sections and is therefore closer to the SEMS reference results. All methods give higher emissions for highway driving than for urban/suburban/rural driving. This is consistent with the SEMS emission results.

The average PN<sub>@90</sub>/CO<sub>2</sub> emission ratios are shown in Fig. 8 on the right. On-board TEN PN23 measurements are displayed in orange. The TEN PN23 results are shown on the secondary axis in Fig. 8 due to the different scale of PN23 compared to PN@90. Plume Chasing real traffic PN@90 results of the VW Caddy show higher emissions than the PN@90 test track measurements (Fig. C.16). The median emissions from e.g. the urban/suburban/rural section (48  $\cdot\,10^{10}\,\text{\# kg}_{\text{fuel}}$ ) are about  $50\,\%$ higher than those of the VW Caddy on the test track  $(30 \cdot 10^{10} \, \text{# kg}_{\text{fuel}})$ Table 5, RolMin method). As expected, the RolMinInd method shows higher emission levels than the RolMin method. The TEN on-board measurements show no major differences in median emissions between urban/suburban/rural driving and highway driving, whereas the PN@90 emissions determined by Plume Chasing are higher by a factor of about 2.7 for highway driving. This could be due to increased interference from other vehicles, from non-exhaust particles (brake wear, re-suspended particles from the road surface) or from other emission sources. As  $PN_{@90}$  and  $PN_{23}$  are not directly comparable, differences could also be due to differences in the particle size distribution (PN@90 measures only particles with a mobility diameter of approximately 90 nm) or to some extent due to a different semi-volatile fraction (which is part of PN@90 but removed in PN23), e.g. due to rapid formation of semi-volatile particles from precursors immediately after exiting the tailpipe (Karjalainen et al., 2019). Further Plume Chasing studies using instruments and on-board measurements that measure the same parameter (e.g. same metric and/or same size range) are needed to better investigate which of the methods is more suitable to reliably measure vehicle PM emissions.

#### 3.4. High-emitter identification

#### 3.4.1. Tampered SCR system

An important application of Plume Chasing is the high-emitter identification. The Plume Chasing NO<sub>x</sub> thresholds for a tampering classification are approximately two (suspicious emitter) to three (highemitter) times higher than the official type approval Euro emission standards. These Plume Chasing thresholds were optimised in previous studies (e.g. Pöhler, 2021) to avoid false positives and to minimise false negatives. With these thresholds, the RolMin method was used to successfully evaluate the SCR status (tampered/non-tampered) of the Ford truck, VW Caddy and VW Transporter on the test track. The onboard SEMS NO<sub>x</sub>/CO<sub>2</sub> emission ratios of the HDV (Ford truck) and two LDVs (VW Caddy and VW Transporter) are shown in Fig. 9 on the left and for Plume Chasing on the right. The measurements are divided between sessions where the SCR system was non-tampered (blue) and where it was tampered (green). Sessions in which the tampering status was just changed leading to unexpected emission values for the SCR state are excluded. This occurred due to the study design, but would not occur in real traffic. Cold SCR situations are also excluded as the emissions change due to SCR warm-up. Plume Chasing can identify such SCR warm-ups from the time series but this cannot be reflected in the averages. In real driving cold SCR systems can be avoided by choosing an appropriate measurement location. The SCR state of both, HDV and VW Transporter, can clearly be separated based on the emission measurements of SEMS. The SCR status of the VW Caddy cannot always be clearly separated because the measured emission distributions of the VW Caddy with and without manipulated SCR for SEMS and Plume Chasing overlap. With the set thresholds no false positive high-emitters are determined in non-convoy driving by Plume Chasing. In convoy driving, LDVs are incorrectly classified as high emitters when a high emitting HDV is driving in front (outliers of VW Transporter). Such situations should be avoided or it must be validated that the vehicle in front is not an interfering high-emitter (see Section 3.2.5). For a more detailed description of the results, also in comparison to the other Remote Emission Sensing Techniques, see Farren et al. (2022b).

#### 3.4.2. Tampered DPF system

In about half of the sessions, the DPF of the VW Caddy was tampered (bypass open). The  $PN_{10}/CO_2$  emission ratios determined by on-board measurements of the NanoMet3 (Fig. 10, left) show that the two tampering states can be clearly separated. The median  $PN_{10}/CO_2$  emission ratios with tampered DPF are about 4 times higher than those with

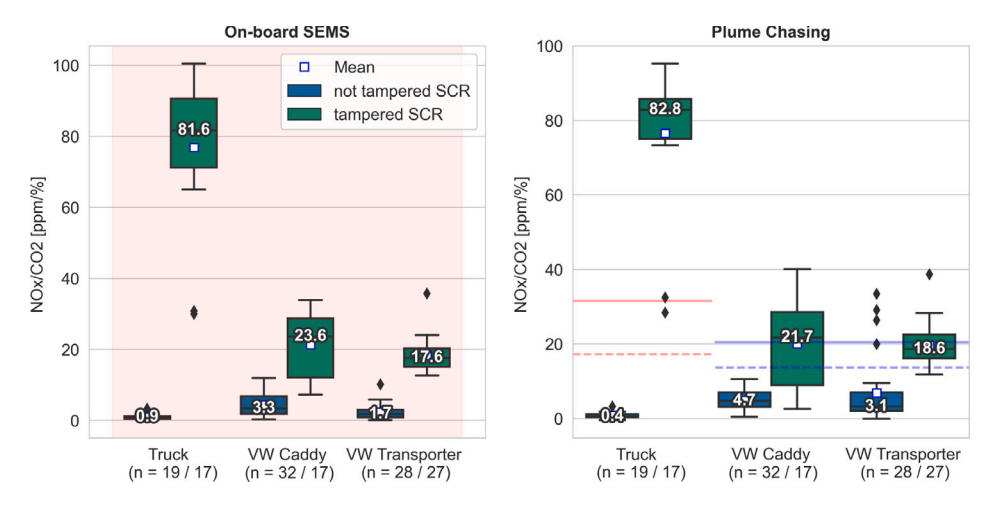


Fig. 9.  $NO_x/CO_2$  emission ratios of HDV (Ford truck) and two LDVs (VW Caddy and VW Transporter) with tampered SCR (green) and non-tampered SCR (blue) determined by on-board SEMS measurements (left) and Plume Chasing (right, determined by *RolMin*). The suspicious (dashed) and high-emitter (solid) thresholds for Euro 6 vehicles are shown in red for the HDV and blue for the LDVs in the right panel. The average SEMS  $NO_x/CO_2$  values are corrected by a factor of 35 % (see Section 3.2.5). The whiskers represent the 1.5 interquartile range (IQR). (For interpretation of the references to colour in this figure legend, the reader is referred to the web version of this article.)

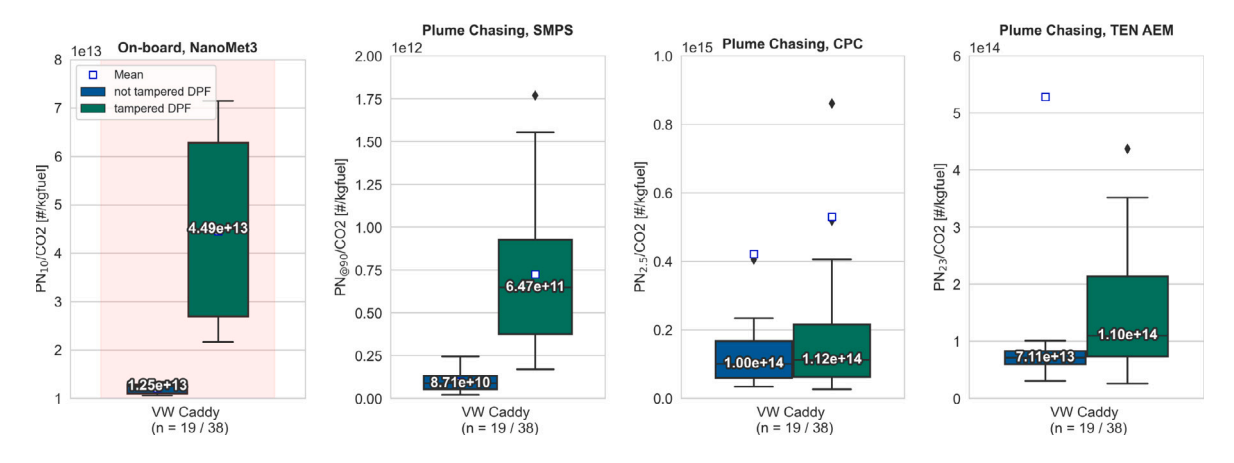


Fig. 10. Distribution of on-board  $PN_{10}/CO_2$  emission ratios measured by NanoMet3 (left), Plume Chasing (determined by RolMinInd)  $PN_{\oplus 90}/CO_2$  (SMPS, middle left),  $PN_{2.5}/CO_2$  (CPC, middle right) and  $PN_{23}/CO_2$  emission ratio (TEN, right) of VW Caddy. The data is divided in sessions with tampered DPF (green) and non-tampered DPF (blue). The whiskers represent the 1.5 interquartile range (IQR). (For interpretation of the references to colour in this figure legend, the reader is referred to the web version of this article.)

non-tampered DPF. This is a rather small difference between tampered and properly functioning DPFs, which are typically about two to three orders of magnitude apart (Boveroux et al., 2019). This is likely because the DPF bypass in this study was too small.

Despite the low PN emissions of the VW Caddy, the SMPS (PN@90) was able to distinguish between sessions with tampered and nontampered DPF (Fig. 10, middle left), whereas the CPC, which measured PN25 (Fig. 10, middle right), could not distinguish between the two states. For the TEN instrument (Fig. 10, right, measuring solid PN23), only a weak differentiation between the two states could be observed. The TEN instrument was optimised for follow-up studies after the test track measurements to improve drifts and noise. The CPC was not suitable for detecting high emitters for several reasons. Firstly, the measurements include volatile compounds which make the results less reproducible (higher uncertainty). Secondly, the CPC uses a size cut-off of 2.5 nm, which can include both core mode and accumulation (soot) mode particles. It is not clear from the literature when non-volatile core mode particles are present, but they are often much more in number than accumulation mode particles and can significantly affect the results for tampered DPF detection (Melas et al., 2021). In addition, CPC measurements were sometimes in the coincidence correction range as no diluter was used, which introduces higher uncertainties. While the measurement of 90 nm particles with the SMPS was useful to correctly determine the tampering status (bypass open/closed) of the VW Caddy,

such a complex measurement system cannot be easily applied for such an application. Other instruments are required to measure particle metrics (e.g. PN, BC) which are suitable for high emitter identification.

#### 3.5. Plume chasing of 2-wheeled vehicles

As part of the test track experiments, two 2-wheeled vehicles were examined to assess the ability of Plume Chasing to determine the emissions of these vehicles. In the setting of the test track experiments the emissions of the 2-wheeled vehicles could be well determined with the investigated methods. The average CO2 value above the lowered threshold of 5 ppm was 14 ppm for the scooter and 21 ppm for the motorcycle (see Fig. E.19 for an example time series of a scooter chase). The NO/CO2 emission ratios of the scooter and motorcycle determined by Plume Chasing are comparable to the on-board Mini-PEMS NO/CO2 emission ratios (Fig. 11). Both methods determined smaller NO emissions of the motorcycle compared to the scooter. The median emissions of the scooter are 1.4 ppm/% lower by Plume Chasing than by on-board measurements, while the median emissions of the motorcycle are 0.5 ppm/% higher. As the measured 2-wheeled vehicles were always measured in a non-convoy situation and the BG was very stable on the test track, no significant effects on the Plume Chasing measurements are expected. Especially for these low emission values, differences may be due to uncertainties in the Mini-PEMS data and also

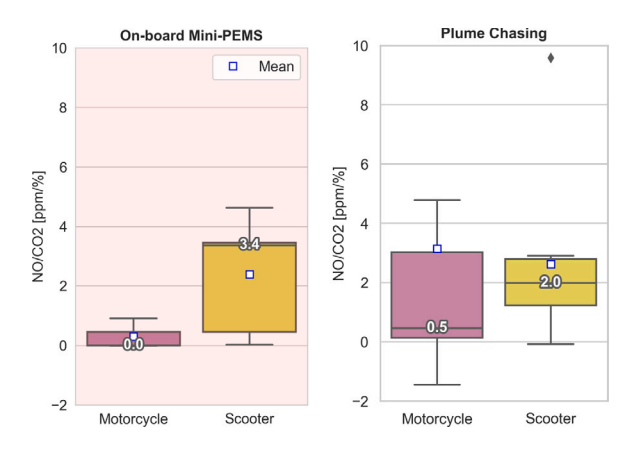


Fig. 11. Average  $NO/CO_2$  emission ratios of the scooter and motorcycle determined by Mini-PEMS (left) and Plume Chasing (right); non-convoy driving. The whiskers represent the 1.5 interquartile range (IOR).

due to data gaps in combination with varying emission ratios.  $PN/CO_2$  emission ratios could also be determined for the 2-wheeled vehicles (Fig. C.16 in the Appendix). PN measurements of the 2-wheelers show increased emissions of sub-23 nm particles.

Difficulties in measuring 2-wheeled vehicles are the small exhaust flow rate and the low absolute emissions (Fig. E.19), which makes it difficult to capture their plume. Therefore, the  $\rm CO_2$  threshold had to be lowered to 5 ppm for the test track data (see Section 2.7) to have enough values for the emission calculation. This makes it difficult to measure 2-wheeled vehicles in dense traffic with many external sources, where even a higher threshold than 20 ppm is recommended. A raised inlet line for Plume Chasing may improve the signal as the exhaust is relatively high up for 2-wheeled vehicles, but this will reduce the signal for other vehicles. Another difficulty is the ability of 2-wheeled vehicles to accelerate very fast. Especially during the high acceleration sessions it was impossible for the slow Plume Chasing vehicle to follow the motorcycle. This could be even more pronounced in real traffic but can be compensated with a smaller and more powerful Plume Chasing vehicle.

#### 4. Conclusions

In this study, we showed optimisation strategies for Plume Chasing to accurately measure vehicle emissions and reliably detect highemitting vehicles. While most of the previous studies have mainly focused on HDVs, we demonstrate the applicability of the Plume Chasing method to LDVs and 2-wheeled vehicles. We designed the study to include convoy driving with different types of vehicles with different levels of  $\mathrm{NO}_{\mathrm{X}}$  emissions, simulating normal traffic situations with low and high emitters.

We evaluated and compared different Plume Chasing data processing methods, including different BG correction-based and regression-based approaches. For  $\mathrm{NO_x}$ , the different data processing methods show only a small bias (0.3–4.7 ppm/% on average, 0.6–3.8 ppm/% on median, 95th percentile at around 7–17 ppm/%) and excellent correlation ( $R^2$  between 0.88 and 0.98) to on-board SEMS measurements for a variety of vehicles types. It underlines the robustness and reliability of the Plume Chasing method.

Conclusions from comparing different methods to analysing Plume Chasing data are:

 The methods using a rolling minimum approach (RolMin, RolMin-Sym, RolMinInd) to derive the BG show better performance compared to the regression based methods and are comparable to other BG determination methods. They feature low operational effort and can be applied in real time analysis. For NO<sub>χ</sub>, the best result is obtained if the BG of the pollutant is taken at the same time as for  $CO_2$ .

- The rolling (*RolReg*) and robust regression (*RobReg*) methods depend on the stringency of the used filters. The results depend on the optimised parameters for the specific purpose. The high requirement on the well matched response of the different measured parameters makes its application more complex but the methods do not require any BG determination. The *RolReg* method can also be applied to real-time data analysis.
- The linear and robust regression method can cause significant wrongly derived emission values if the ratio of the pollutant to CO<sub>2</sub> changes over the measurement period, e.g. due to an engine change or a change in the SCR efficiency. In an example of such a case, method *LinReg* underestimated the emissions by 50%, *RobReg* by 75%. This problem can be reduced with the short duration rolling regression method as it can account for changes in the ratio of pollutant to CO<sub>2</sub> throughout a plume chase.
- There is no significant observed difference (±1%) between determining BG from a BG interval symmetrically or backwards from the point of measurement (*RolMin* or *RolMinSym*). The change in the length of the interval in which the BG is determined plays a greater role. If a BG interval of 480s is used instead of 120s, the emission ratios are on average up to 9% lower and 9% higher for 60s.
- The method using an additional measurement on the roof of the chasing vehicle (BGinlet) performs slightly better for measuring LDVs behind high-emitting HDVs or in heavy traffic situations. Instead of ~ 35 %, the influence of the HDV can be reduced to about ~ 24 %. However, performing a second measurement on the roof is very costly compared to the relatively small improvement in data quality. Whether this is worthwhile depends on the application.
- For PN emissions, the *RolMinInd* method of searching for CO<sub>2</sub> and PN BG individually is advantageous as long as the influence of other emission sources is small. The method is more appropriate because PM and gaseous emissions can occur at different times. The derived emission values are on average higher and the data processing method may cause an overestimation. How much depends strongly on the measured metric and on other interfering emission sources. Further research is needed to determine which particle metric (e.g. PN, BC) is most appropriate for identifying high emitters.
- The average absolute deviation of the determined  $NO_x/CO_2$  emission ratios (using the *RolMin* method) from the reference was  $-0.2(46)\,\mathrm{ppm/\%}$  for the HDV and  $0.3(29)\,\mathrm{ppm/\%}$  for the LDVs tested (non-convoy driving). The average absolute deviation of the determined  $NO/CO_2$  ratio for the two-wheeled vehicles was  $0.2(27)\,\mathrm{ppm/\%}$ .

Plume Chasing measurements can be influenced by other emission sources and other vehicle plumes. From convoy driving we estimated the influence of different emission sources. A high-emitting LDV in front of a low-emitting vehicle have a moderate influence of up to 22 % on the measured emission levels. Around 35 % of the measured emission signal of a low-emitting LDV can come from a high-emitting HDV driving directly in front of it. Such interfering plumes from high-emitters can lead to false positive detection for LDVs. We suggested strategies to avoid them. Apart from those situations Plume Chasing was able to distinguish reliably between tampering and non-tampering of the different vehicles tested (no false positives). The RolMin method has proven effective in identifying high-emitters in real-time. We showed that high PM emitters can be effectively identified using SMPS 90 nm data in a Plume Chasing setup and correlate well with on-board measurements. The data from a CPC shows none, and the data of the TEN AEM only slight separation between low and high PM emitter states. Further research is needed to develop a reliable, simpler and less expensive approach to PM measurement. The combination of an ICAD and a suitable PM measurement instrument can provide a simple setup for Plume Chasing and robust and reliable high-emitter identification for NO<sub>x</sub> and PM emissions.

Table A.6
Weather conditions during the test track measurement campaign. Averages are calculated for the time of measurement.

Date	T [°C]	v <sub>wind</sub> [m/s]	Wind direction	RH [%]
21.06.2021	15.0	10.7	NE	89.2
22.06.2021	16.0	11.3	NE	68.6
23.06.2021	15.8	7.1	NE to SE	69.3
24.06.2021	16.2	6.1	NE to SE	70.7
25.06.2021	15.5	7.8	SW	80.1

#### CRediT authorship contribution statement

Schmidt Christina: Writing – review & editing, Writing – original draft, Visualization, Software, Methodology, Investigation, Formal analysis, Conceptualization. Carslaw C. David: Writing – review & editing, Project administration. Farren J. Naomi: Writing – review & editing, Validation, Project administration, Investigation, Formal analysis. Gijlswijk N. René: Writing – review & editing, Resources, Investigation. Knoll Markus: Writing – review & editing, Resources, Investigation. Ligterink E. Norbert: Resources, Project administration. Lollinga Jan Pieter: Resources, Investigation. Pechout Martin: Resources, Investigation. Schmitt Stefan: Software. Vojtíšek Michal: Writing – review & editing, Validation, Resources, Investigation. Vroom Quinn: Resources, Project administration, Investigation. Pöhler Denis: Writing – review & editing, Validation, Supervision, Resources, Project administration, Methodology, Investigation, Funding acquisition, Conceptualization.

#### Declaration of competing interest

The authors declare that they have no known competing financial interests or personal relationships that could have appeared to influence the work reported in this paper.

#### Acknowledgements

This study was conducted under the European project City Air Remote Emission Sensing (CARES), which has received funding from the European Union's Horizon 2020 research and innovation program under grant agreement No. 814966. We acknowledge all project partners for their help during sampling and/or analysis. We would especially like to thank Åke Sjödin (IVL) for his great support throughout the project and Prof Ulrich Platt for his supervision and valuable feedback on this manuscript.

#### Appendix A. Measurement conditions

The average ambient air temperature, wind speed, direction and relative humidity for the days of the test track measurements can be found in Table A.6. The temperature was similar on all measurement days ( $\approx 16$  °C), whereas the wind speed was stronger during the first two days ( $\approx 11 \text{ m/s}$ ) than during the remaining three days ( $\approx 7 \text{ m/s}$ ). There was no precipitation on the days of measuring and the relative humidity was about 70 to 90 %.

The test route of real traffic measurements is shown in Fig. A.12.

#### Appendix B. Measurement setups

The used Plume Chasing vehicle from TNO is shown in Fig. B.13 with its inlets (two at the front and one on the roof of the vehicle).

The Mini-PEMS were installed on the luggage rack of the motorcycles (see Fig. B.14).

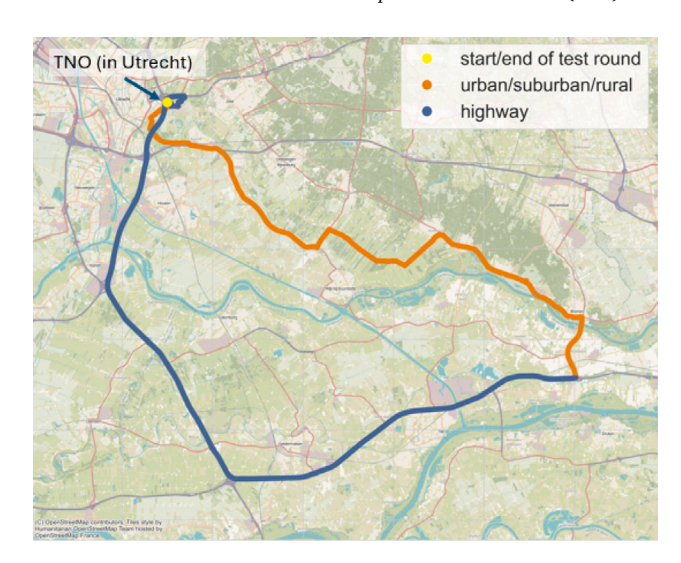


Fig. A.12. Test route, urban/suburban/rural segments marked in orange, highway segments in blue. The start/end point at TNO in Utrecht is marked in yellow. (For interpretation of the references to colour in this figure legend, the reader is referred to the web version of this article.)



Fig. B.13. Plume Chasing vehicle.





Fig. B.14. Mini-PEMS installed on the Yamaha MT-07 Motorcycle (left) and Yamaha NMAX Scooter (right).

### Appendix C. Average $NO_x/CO_2$ and $PN/CO_2$ ratios of different vehicles and instruments

The  $\mathrm{NO_x/CO_2}$  and  $\mathrm{PN_{10}/CO_2}$  emission ratios determined from onboard reference (SEMS and NanoMet3) as well as Plume Chasing measurements separated into convoy and non-convoy data are shown in Table C.7. The average  $\mathrm{NO_x/CO_2}$  emission ratios of all investigated vehicles determined by the *RolMin* Plume Chasing method can be found in Fig. C.15.

The average  $PN/CO_2$  emission ratios ( $PN \in [PN_{@90}, PN_{23}, PN_{2.5}]$ ) of all investigated vehicles determined by the *RolMinInd* Plume Chasing method can be found in Fig. C.16.

Table C.7 Mean and Median  $NO_x/CO_2$  and  $PN_{10}/CO_2$  emission ratios determined from on-board reference (SEMS and NanoMet3) as well as Plume Chasing (RolMin) measurements of the Ford truck, VW Caddy and VW Transporter. Separated into convoy and non-convoy data.

			Ford truck	VW Caddy	VW Transporter	VW Caddy
On-board			NO <sub>x</sub> /CO <sub>2</sub> [ppr	m/%]		$PN_{10}/CO_2 \ [\#/kg_{fuel}] \cdot 10^{13}$
Convoy	Tampered	Mean Median	81.9 ± 17.4 79.3	$26.8 \pm 6.4$ 28.7	$18.1 \pm 2.2$ 17.7	$3.8 \pm 1.7$ 3.0
Convoy	Non-tampered	Mean Median	$0.7 \pm 0.4$ 0.9	$3.1 \pm 2.3$ 2.5	$3.0 \pm 2.7$ 2.6	$1.33 \pm 0.02$ 1.3
Non-convoy	Tampered	Mean Median	75.7 ± 21.3 82.5	19.1 ± 9.8 20.2	18.3 ± 5.4 17.6	5.1 ± 1.8 4.8
Non-convoy	Non-tampered	Mean Median	$1.0 \pm 0.9$ 0.9	$5.1 \pm 3.3$ 5.2	$1.8 \pm 1.5$ $1.5$	$1.2 \pm 0.1$ 1.2
Plume Chasing	Plume Chasing (RolMin)		$NO_x/CO_2$ [ppm/%]			$PN_{@90}/CO_2 \ [\#/kg_{fuel}] \cdot 10^{10}$
Convoy	Tampered	Mean Median Mean	$83.8 \pm 11.0$ 83.0 $1.2 \pm 0.5$	$28.7 \pm 6.3$ 32.0 $4.8 \pm 2.1$	$17.0 \pm 3.2$ $16.4$ $12.3 \pm 11.5$	64.7 ± 26.4 65.3 7.6 ± 1.7
	Non-tampered	Median	1.1	4.4	7.0	7.6
Non-convoy	Tampered	Mean Median	$75.0 \pm 19.5$ 81.2	$16.4 \pm 12.3$ $12.9$	$20.6 \pm 6.3$ 21.0	64.9 ± 49.6 44.3
rion convoy	Non-tampered	Mean Median	$0.6 \pm 0.8$ 0.4	$4.9 \pm 3.2$ 5.2	$2.7 \pm 2.3$ 2.2	$3.5 \pm 7.4$ $3.4$

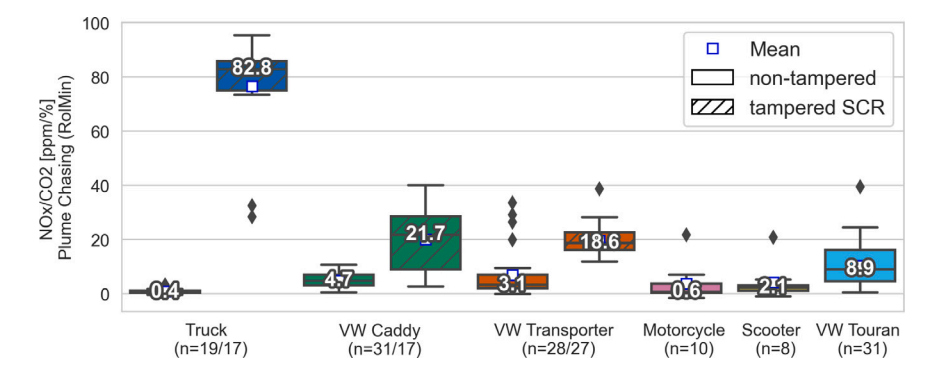


Fig. C.15.  $NO_x/CO_2$  emission ratios of all different vehicles measured by Plume Chasing. The *RolMin* method is used for determining the emission ratios. Sessions in which the tampering status was just changed, as well as cold SCR situations, are excluded.

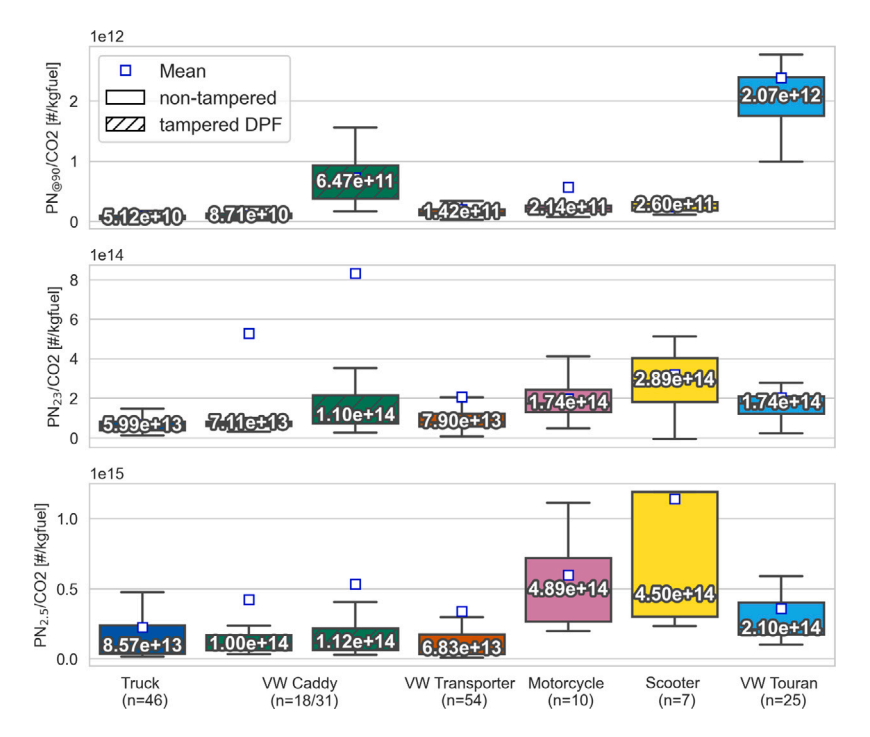


Fig. C.16.  $PN_{@90}/CO_2$  (upper),  $PN_{23}/CO_2$  (middle) and  $PN_{2.5}/CO_2$  (bottom) emission ratios of all different vehicles measured by Plume Chasing. The *RolMinInd* method is used for determining the emission ratios.

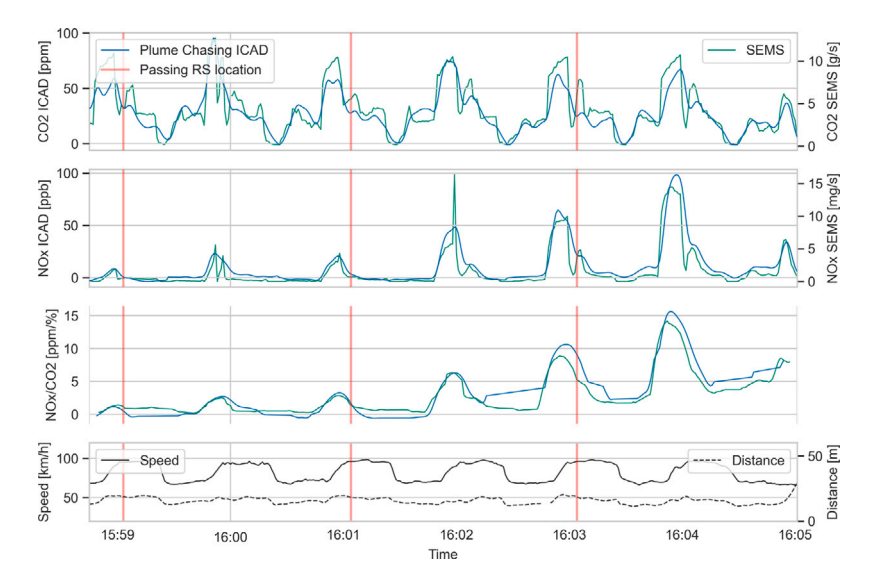


Fig. E.17. Example of synchronised data time series of Plume Chasing and SEMS within a chasing period (three laps) of the VW Caddy. The time series of measured  $NO_x$  and  $CO_2$  of SEMS (green) and Plume Chasing (blue, BG-corrected) are shown in the top two panels, the ratio  $NO_x/CO_2$  (rolling 9 s mean) of SEMS and Plume Chasing and the time series of speed (solid) and distance (dashed) to the chased vehicle in the lower two panels. The red vertical lines mark the passing time at the location of the other remote sensing techniques (Opus RSE/Point Sampling). (For interpretation of the references to colour in this figure legend, the reader is referred to the web version of this article.)

#### Appendix D. Calculations RolMin

The derived BG value used for the emission calculation does not have to be the real BG without the emission, it may still contain some plume emissions that are cancelled out in the calculation. The measured signal of the component  $X_{\text{meas}}(t)$  should be corrected by the background value  $BG_X(t)$  to derive the real plume signal  $X_{\text{plume}}(t)$ . If the used background  $BG_X(t_{\text{min}})$  at time  $t_{\text{min}}$  still contains a part k of the plume signal than the used background would be  $BG_X(t) + k \cdot X_{\text{plume}}(t_{\text{min}})$ . As the fraction of k applies for the pollutant and for  $CO_2$  in the same way, the following generally applies:

$$\begin{split} &\frac{X_{\text{meas}}(t) - BG_{X}(t_{\text{min}})}{CO_{2 \text{ meas}}(t) - BG_{CO_{2}}(t_{\text{min}})} \\ &= \frac{X_{\text{meas}}(t) - [BG_{X}(t) + k \cdot X_{\text{plume}}(t_{\text{min}})]}{CO_{2 \text{ meas}}(t) - [BG_{CO_{2}}(t) + k \cdot CO_{2 \text{ plume}}(t_{\text{min}})]} \\ &= \frac{X_{\text{plume}}(t) - k \cdot X_{\text{plume}}(t_{\text{min}})}{CO_{2 \text{ plume}}(t) - k \cdot CO_{2 \text{ plume}}(t_{\text{min}})} \\ &= \frac{R_{E}(t) \cdot CO_{2 \text{ plume}}(t) - R_{E}(t_{\text{min}}) \cdot k \cdot CO_{2 \text{ plume}}(t_{\text{min}})}{CO_{2 \text{ plume}}(t) - k \cdot CO_{2 \text{ plume}}(t_{\text{min}})} \end{split}$$

If the emission ratio  $R_E$  (and the BG) is constant over the period of the rolling minimum interval, then  $R_E(t_{\min}) = R_E(t)$ . The above equation then gives  $R_E(t)$ , similar to if the background were not contaminated by a remaining plume:

$$= \frac{R_E(t) \cdot \text{CO}_{2 \text{ plume}}(t) - R_E(t) \cdot k \cdot \text{CO}_{2 \text{ plume}}(t_{\text{min}})}{\text{CO}_{2 \text{ plume}}(t) - k \cdot \text{CO}_{2 \text{ plume}}(t_{\text{min}})}$$

$$= R_E(t)$$
(D.2)

#### Appendix E. Plume chasing time series

Fig. E.17 shows an example time series where the Plume Chasing vehicle followed the VW Caddy for three laps at speeds between 70 and  $100\,\mathrm{km/h}$ . The red vertical lines indicate the time at which the location of the other remote sensing techniques (in-situ Point Sampling and cross-road Opus RSE) on the test track was passed. From vertical line to line is therefore one lap. The  $\mathrm{NO_x}$  emissions increase from lap to lap because the SCR has just been switched off before the measurement and it takes some time for the remaining Adblue to be used up and the

emissions to increase.

Fig. E.18 shows an example time series where, without a speed filter, the plume from the measurement vehicle itself (Plume Chasing  ${\rm CO_2}$  and  ${\rm NO_x}$  data in the red shaded area) would be part of the emission ratio determination. The SEMS data of the chased HDV shows that there were no emissions from the HDV at the relevant time.

Fig. E.19 shows an example time series of the scooter's  $\rm CO_2$  and NO emissions measured by the on-board Mini-PEMS (green line) and Plume Chasing (blue line).

Fig. E.20 shows an example time series of  $CO_2$ ,  $NO_x$  and  $PN_{@90}$  with the determined BG time series of method *RolMin* (green) and *RolMinInd* (orange).

#### Appendix F. Absolute deviation to SEMS - separated by vehicle

The distribution of the absolute deviation of  $NO_x/CO_2$  Plume Chasing to SEMS emission ratios for the different data processing methods and tested vehicles for convoy data only is displayed in Fig. F.21. In Fig. F.22 the absolute deviation of convoy and non-convoy data is shown for the Ford truck, in Fig. F.23 for the VW Caddy and Fig. F.24 for the VW Transporter.

## Appendix G. Influence of speed filter, smoothing and the $\mathrm{CO}_2$ sensor

#### G.1. Speed filter

Analysis of parameters such as speed, acceleration or distance to the chased vehicle showed that filters such as a speed filter ( $v > 10\,\mathrm{km/h}$ ) can improve the determination of emission ratios. Fig. E.18 shows an example time series where, without a speed filter, the plume from the own measurement vehicle contaminate the observed emission ratio. If the chased vehicle is surrounded by other vehicles in real traffic conditions (e.g. at a traffic light), the plume from other vehicles could affect the measurements in the same way. The extent to which this can affect the measurement depends mainly on the wind conditions and the type of nearby/chasing vehicle (low-emission or electric vehicles would have little effect on the measurements).

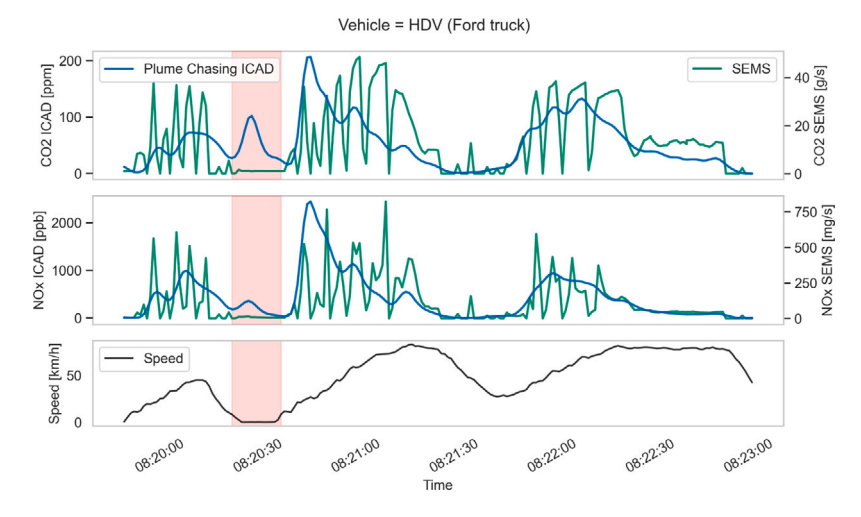


Fig. E.18. Time series of  $CO_2$  and  $NO_\chi$  measured by Plume Chasing and SEMS of the truck, one lap. The red shaded area marks the chasing time with a chasing velocity <  $10 \, km/h$ . (For interpretation of the references to colour in this figure legend, the reader is referred to the web version of this article.)

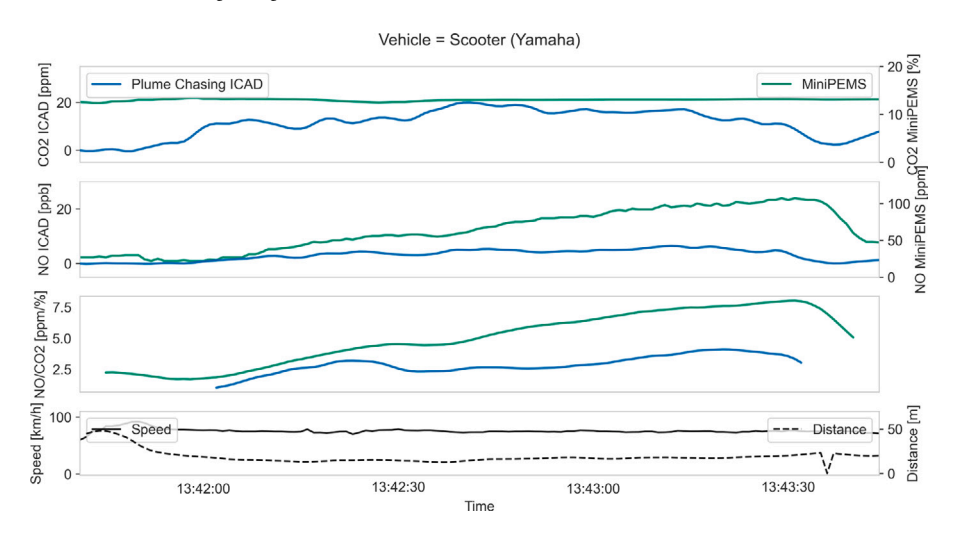


Fig. E.19. Example time series of CO2 and NO from Plume Chasing and Mini-PEMS measurements of the scooter. Non-convoy driving.

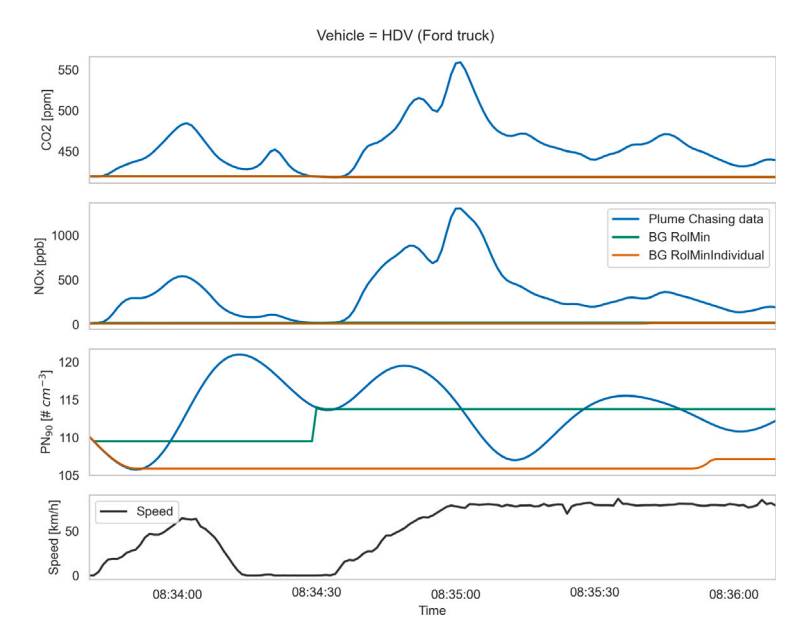


Fig. E.20. Example time series of  $CO_2$ ,  $NO_x$  and  $PN_{@90}$  with BG time series of method *RolMin* and *RolMinInd*.

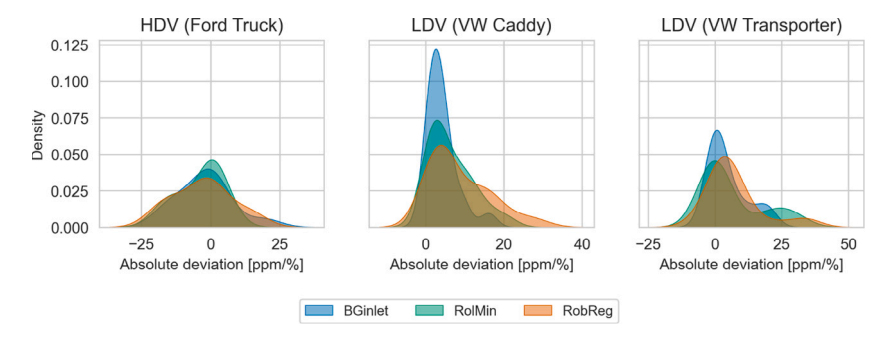


Fig. F.21. Distributions of the absolute deviations of  $NO_x/CO_2$  Plume Chasing to SEMS emission ratios of the methods BGinlet, RolMin and RobReg for the Ford truck (left), VW Caddy (middle) and VW Transporter (right). Only convoy data is included.

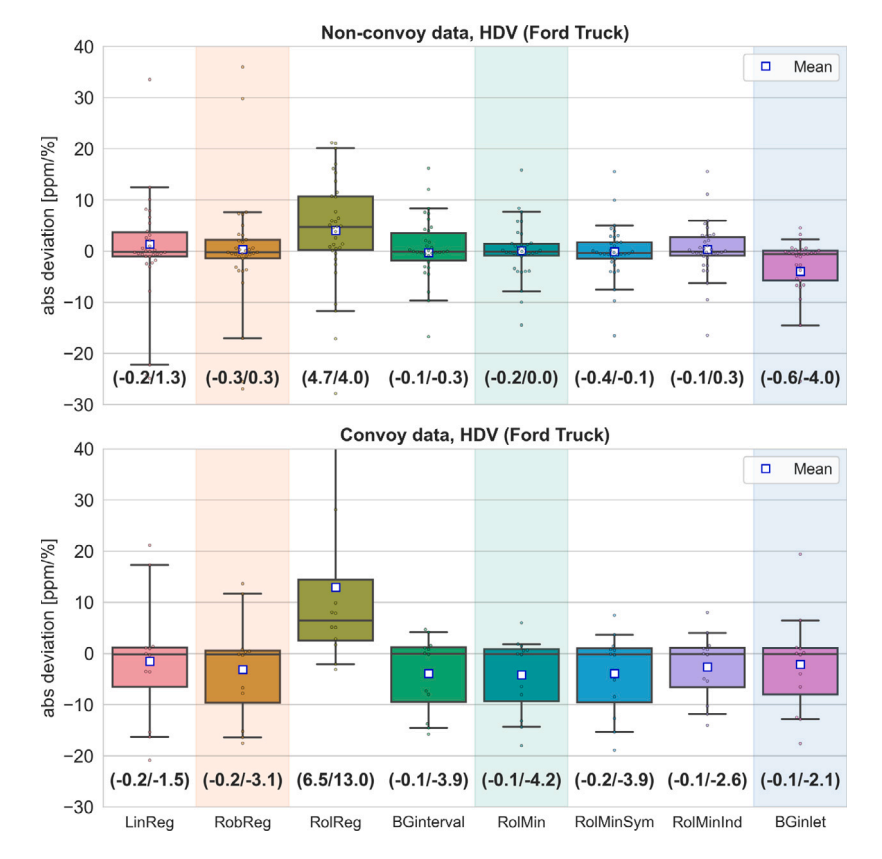


Fig. F.22. Comparison (absolute deviations) of  $NO_x/CO_2$  Plume Chasing and SEMS of different methods for a HDV (Ford truck); top: convoy driving, bottom: non-convoy driving. The median/mean absolute deviation of each method is given in brackets below each box-plot. The whiskers represent the 5th and the 95th percentiles.

#### G.2. Smoothing

Smoothing the data, i.e. reducing the time resolution, may improve the result by reducing the sensitivity to, for example, the different response times of instruments (Xiang et al., 2023; Wang et al., 2020). For the data from the test track, a 5s-average was tested, but no improvements were found. This could be due to the fact that we have optimised the time synchronisation and instrument response time correction as described in Section 2.3, as well as the instrumentation for this type of measurement.

#### G.3. LI-COR 7000 $CO_2$ sensor

A main requirement is a fast response time of the analysers of better 5 s. A response time and resolution of 2 s like for the used ICAD instruments is recommended. We found that the medium-cost  $\rm CO_2$  sensor used in the ICAD with a slope accuracy of 1 % (+ absolute error of 20 ppm) correlates well with high-precision  $\rm CO_2$  sensors with absolute

Table H.8 VW Transporter  $NO_x/CO_2$  emission ratios determined by different Plume Chasing methods and SEMS for a chase on 22.06.2021.

	SEMS	LinReg	RobReg	RolMin
NO <sub>x</sub> /CO <sub>2</sub> [ppm/%]	21.1	21.4	21.3	22.0

error of 1% (e.g. LI-COR, see Fig. G.25). The use of medium-cost  $\mathrm{CO}_2$  sensors in applications such as Plume Chasing or Point Sampling is therefore feasible, as only negligible differences in calculated emission factors were found compared to high grade instruments (see also Sugrue et al., 2020).

#### Appendix H. Linear and robust regression

An example where both the *LinReg* and *RobReg* method give average emission ratios close to the SEMS emission ratios is illustrated for one chase of the VW Transporter (Fig. H.26). The ratio of  $NO_x$  to  $CO_2$  is

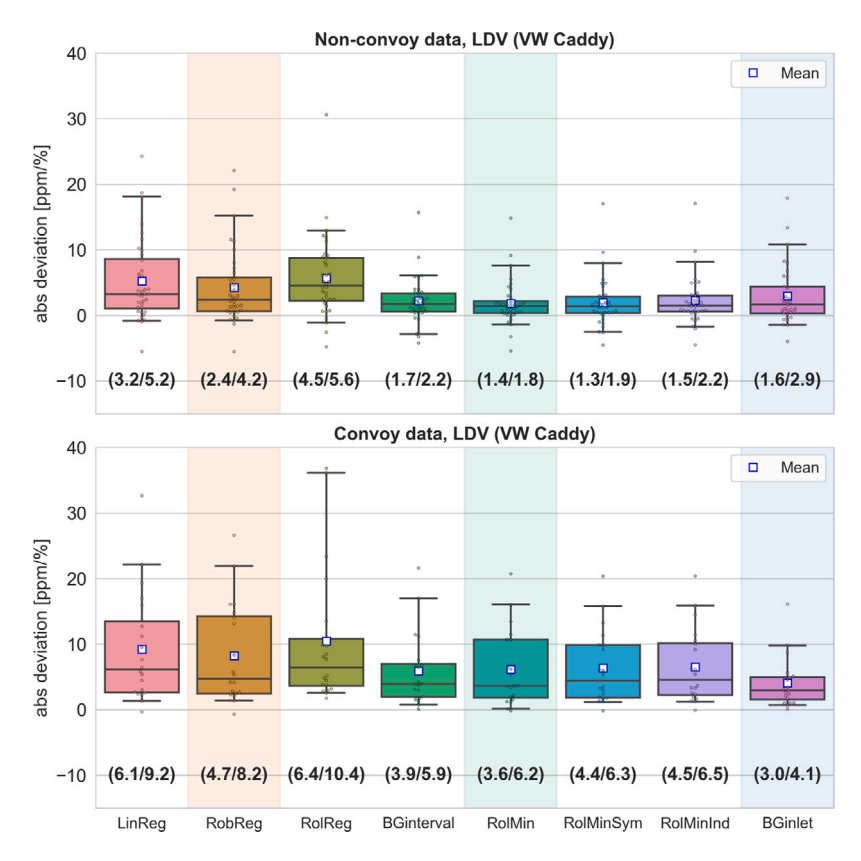


Fig. F.23. Comparison (absolute deviations) of NO<sub>x</sub>/CO<sub>2</sub> Plume Chasing and SEMS of different methods for a LDV (VW Caddy); top: convoy driving, bottom: non-convoy driving. The median/mean absolute deviation of each method is given in brackets below each box-plot. The whiskers represent the 5th and the 95th percentiles.

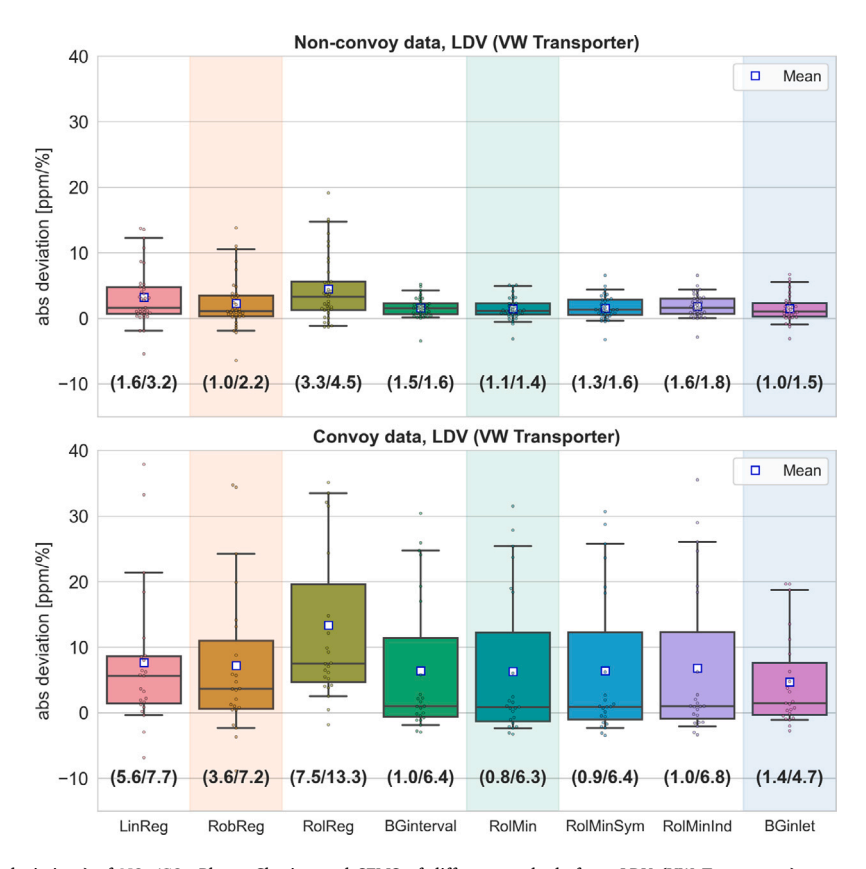


Fig. F.24. Comparison (absolute deviations) of  $NO_x/CO_2$  Plume Chasing and SEMS of different methods for a LDV (VW Transporter); top: convoy driving, bottom: non-convoy driving. The median/mean absolute deviation of each method is given in brackets below each box-plot. The whiskers represent the 5th and the 95th percentiles.

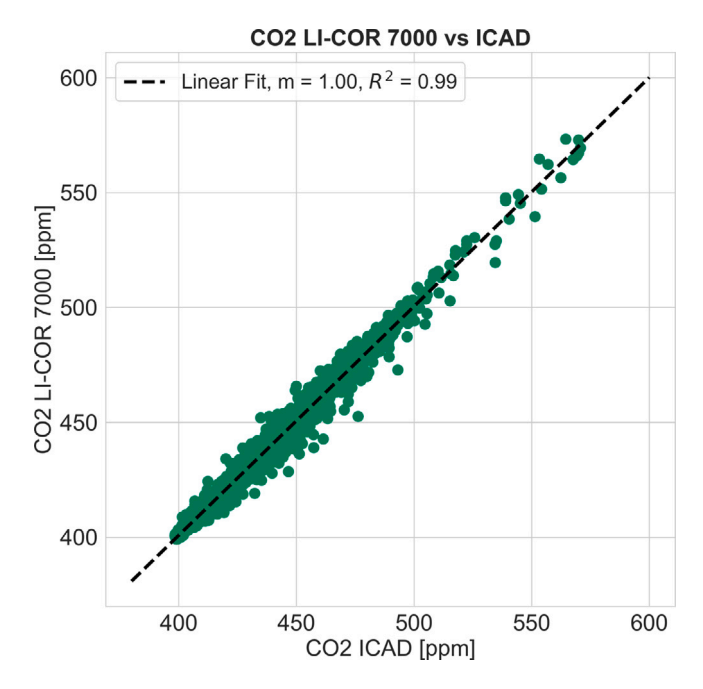


Fig. G.25. Comparison of CO2 measured by a LI-COR 7000 and ICAD-NOx-150DE-M instrument (Airyx GmbH). The data is shown for one day of measurements.

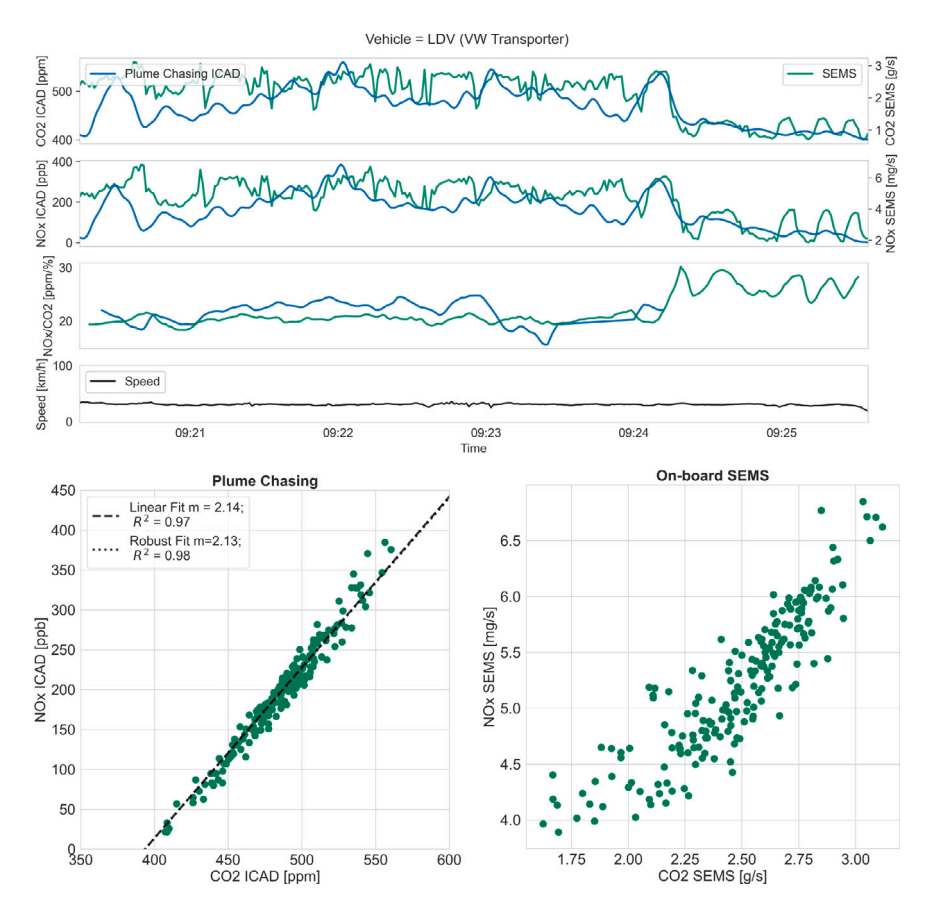


Fig. H.26. Time series (top) of  $CO_2$  and  $NO_x$  measured by Plume Chasing (blue) and SEMS (green), one lap, chased vehicle was the VW Transporter. The  $NO_x$  data are plotted against the  $CO_2$  data for the Plume Chasing measurements on the bottom left and for the SEMS measurements on the bottom right. Regression lines of the methods LinReg (dashed black line) and RobReg (dotted black line) are shown. (For interpretation of the references to colour in this figure legend, the reader is referred to the web version of this article.)

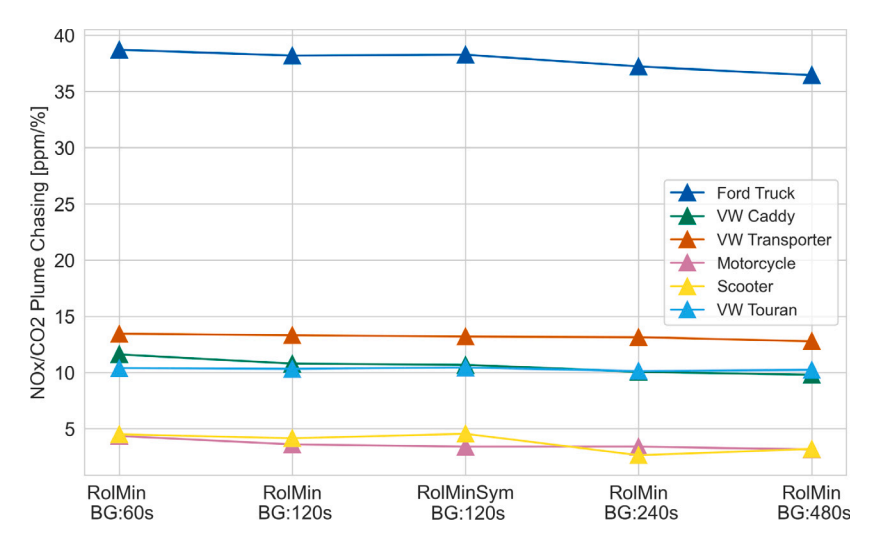


Fig. 1.27. Comparison of average  $NO_x/CO_2$  emission ratios of different BG intervals (60 s, 120 s, 240 s and 480 s) for the *RolMin* method. The average emission ratios of the *RolMinSym* method (symmetrically  $\pm 60$  s) are also displayed. The results are plotted separately for all vehicles.

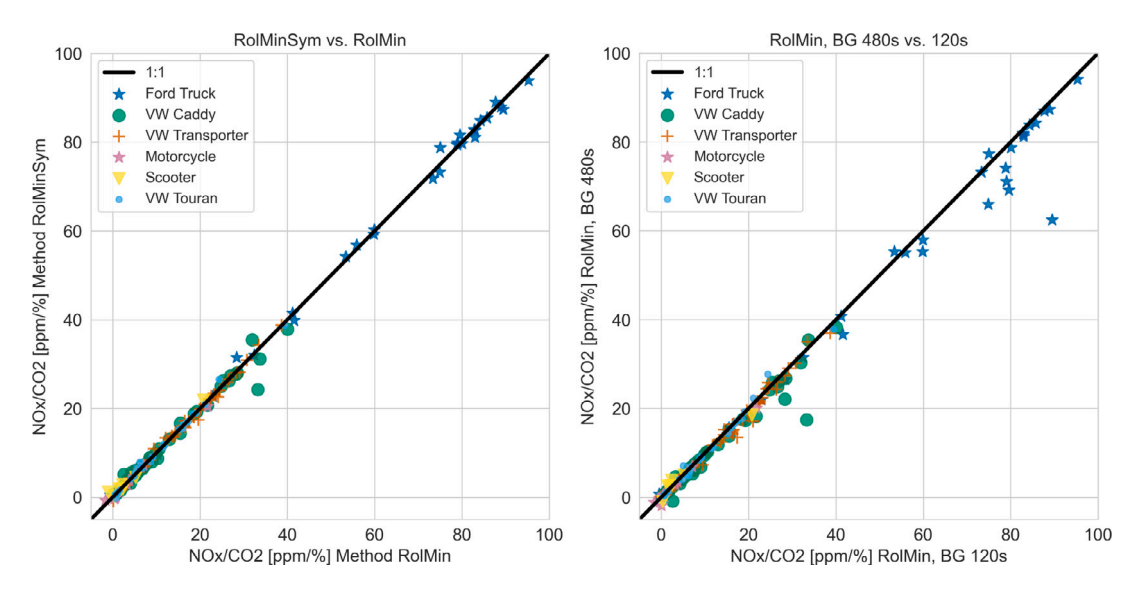


Fig. 1.28. Comparison of  $NO_x/CO_2$  emission ratios of methods *RolMin* vs *RolMinSym* for all vehicles (left) and of different BG intervals (480 s vs 120 s) for the method *RolMin* (right) for all vehicles.

constant over time. The methods *RolMin*, *LinReg* and *RobReg* are all close to the SEMS emission ratio of 21.1 ppm/% with 22.0, 21.4 and 21.3 ppm/% respectively (see Table H.8).

#### Appendix I. Robustness of RolMin

In Fig. I.27 the average  $NO_x/CO_2$  emission ratios of different BG intervals (60 s, 120 s, 240 s, 480 s backward or  $\pm 60$  s symmetrical) show, that the exact BG interval used for the BG search does not change the results significantly.

In Fig. I.28 (left) the average emission ratios obtained by the *RolMinSym* method are plotted against those obtained by the *RolMin* method. Each data point is the derived emission value of one driving constellation, typically one lap (2.8 km). In Fig. I.28 (right) the average emission ratios determined from the *RolMin* method with a BG interval of  $480\,\mathrm{s}$  is compared to the one with a BG interval of  $120\,\mathrm{s}$ . The comparisons show that only few data points deviate by  $10–20\,\mathrm{ppm}/\%$ , all others are in good agreement.

#### Appendix J. Convoy vs non-convoy driving

A scatter plot of the derived  $\mathrm{NO_x/CO_2}$  ratios of Plume Chasing calculated with the *BGinlet* method against those of SEMS is shown in Fig. J.29 for the Ford truck (left), the VW Caddy (middle) and the VW Transporter (right). Compared to other Plume Chasing data processing methods, the average emissions show lower deviations to the SEMS values in situations where a high-emitting HDV is driving in front of a low emitting LDV (e.g. triangular orange dots). However, the underestimation of the HDV emission ratios by the *BGinlet* method is also clearly visible.

#### Appendix K. Comparison of RolMinInd and RolMin

The PN<sub>@90</sub>/CO<sub>2</sub> emission ratios of the *RolMinInd* and the *RolMin* method are compared in Fig. K.30.

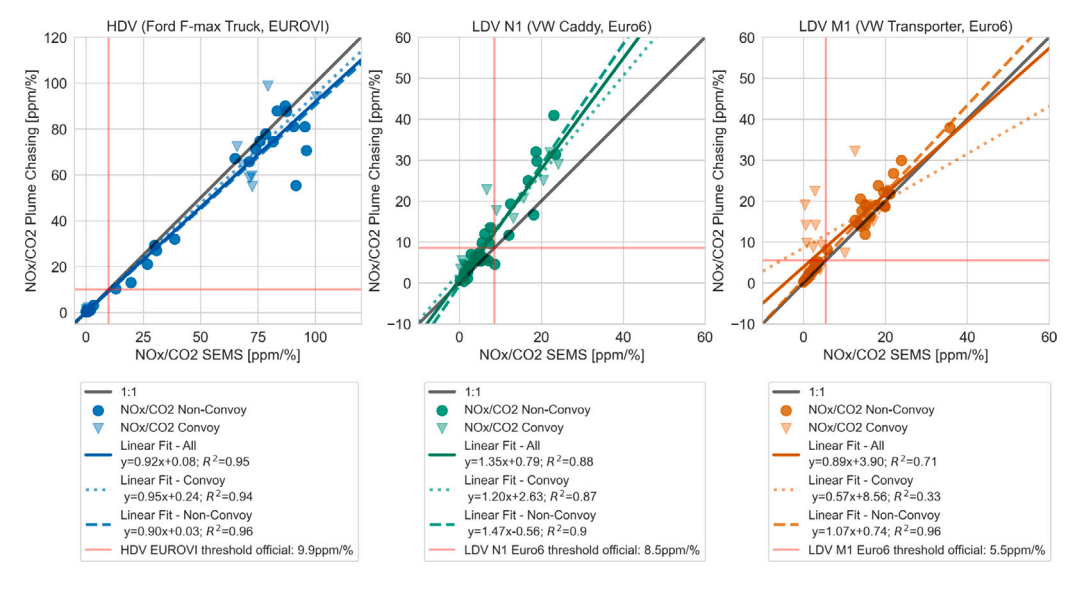


Fig. J.29. Scatter plot NO<sub>x</sub>/CO<sub>2</sub> Plume Chasing (BGinlet) vs. SEMS of Ford truck (left), VW Caddy (middle) and VW Transporter (right). Each data point is the derived emission value of one driving constellation, typically one lap (2.8 km).

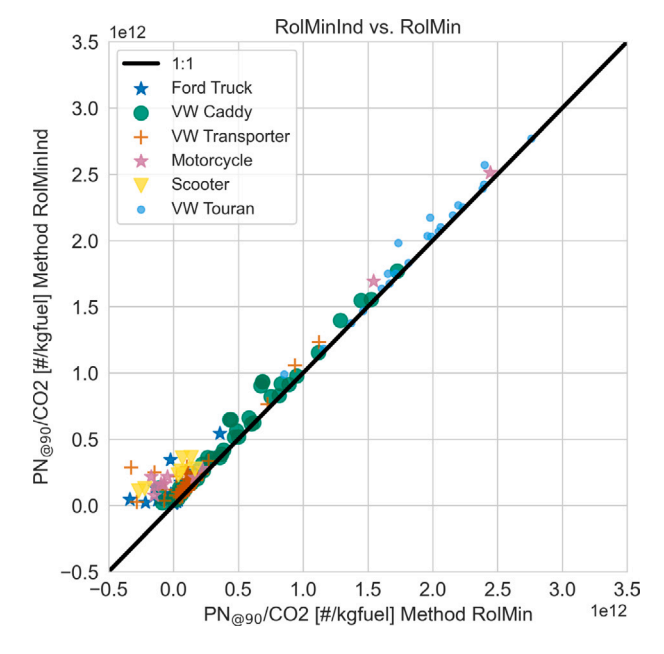


Fig. K.30. Comparison of  $\mathrm{PN}_{\oplus 90}/\mathrm{CO}_2$  emission ratios of the *RolMinInd* method vs the *RolMin* method.

#### Data availability

Data will be made available on request.

#### References

Bishop, G.A., Starkey, J.R., Ihlenfeldt, A., Williams, W.J., Stedman, D.H., 1989. Ir long-path photometry: A remote sensing tool for automobile emissions. Anal. Chem. 61 (10), 671A–677A. http://dx.doi.org/10.1021/AC00185A002.

Boveroux, F., Cassiers, S., Buekenhoudt, P., Chavatte, L., Meyer, P.D., 2019. Feasibility study of a new test procedure to identify high emitters of particulate matter during periodic technical inspection. SAE Tech. Pap. 2019–01–1190. http://dx.doi.org/10. 4271/2019-01-1190.

Burtscher, H., Lutz, T., Mayer, A., 2019. A new periodic technical inspection for particle emissions of vehicles. Emiss. Control. Sci. Technol. 5 (3), 279–287. http: //dx.doi.org/10.1007/S40825-019-00128-Z. Canagaratna, M.R., Jayne, J.T., Ghertner, D.A., Herndon, S., Shi, Q., Jimenez, J.L., Silva, P.J., Williams, P., Lanni, T., Drewnick, F., Demerjian, K.L., Kolb, C.E., Worsnop, D.R., 2004. Chase studies of particulate emissions from in-use new york city vehicles. Aerosol Sci. Technol. 38 (6), 555–573. http://dx.doi.org/10.1080/02786820490465504.

Farren, N., Carslaw, D., Knoll, M., Schmidt, C., Pöhler, D., Hallquist, A., 2022a. City Air Remote Emission Sensing (CARES) EU Horizon 2020 Project: Deliverable 1.1 Measurement technology intercomparison and evaluation. Technical Report, CARES, URL https://cares-project.eu/measurement-tech-compare-d1-1/.

Farren, N., Carslaw, D., Knoll, M., Schmidt, C., Pöhler, D., Hallquist, A., 2022b. City Air Remote Emission Sensing (CARES) EU Horizon 2020 Project: Deliverable 1.2 Monitoring of vehicle tampering. Technical Report, CARES, URL https://cares-project.eu/monitoring-vehicle-tampering-d1-2/.

Farren, N.J., Schmidt, C., Juchem, H., Pöhler, D., Wilde, S.E., Wagner, R.L., Wilson, S., Shaw, M.D., Carslaw, D.C., 2023. Emission ratio determination from road vehicles using a range of remote emission sensing techniques. Sci. Total Environ. 875, 162621. http://dx.doi.org/10.1016/J.SCITOTENV.2023.162621.

Fiebig, M., Wiartalla, A., Holderbaum, B., Kiesow, S., 2014. Particulate emissions from diesel engines: correlation between engine technology and emissions. J. Occup. Med. Toxicol. 9 (1), 6. http://dx.doi.org/10.1186/1745-6673-9-6.

Hansen, A.D., Rosen, H., 1990. Individual measurements of the emission factor of aerosol black carbon in automobile plumes. J. Air Waste Manage. Assoc. 40 (12), 1654–1657. http://dx.doi.org/10.1080/10473289.1990.10466812.

Herndon, S.C., Shorter, J.H., Zahniser, M.S., Wormhoudt, J., Nelson, D.D., Demerjian, K.L., Kolb, C.E., 2005. Real-time measurements of SO2, H2CO, and CH4 emissions from in-use curbside passenger buses in new york city using a chase vehicle. Environ. Sci. Technol. 39 (20), 7984–7990. http://dx.doi.org/10.1021/F50482942.

Horbanski, M., Pöhler, D., Lampel, J., Platt, U., 2019. The ICAD (iterative cavity-enhanced DOAS) method. Atmospheric Meas. Tech. 12 (6), 3365–3381. http://dx.doi.org/10.5194/amt-12-3365-2019.

Horizon, 2020. CARES | City Air Remote Emission Sensing. http://dx.doi.org/10.3030/814966, URL https://cares-project.eu/.

Janssen, J., Hagberg, N., 2020. Plume Chasing - A way to detect high NOx emitting vehicles. Technical Report, https://www.danishroadtrafficauthority.dk/Media/638350311390689301/PlumeChasing-AwaytodetecthighNOxemittingvehicles.pdf.

Ježek, I., Drinovec, L., Ferrero, L., Carriero, M., Močnik, G., 2015. Determination of car on-road black carbon and particle number emission factors and comparison between mobile and stationary measurements. Atmospheric Meas. Tech. 8 (1), 43–55. http://dx.doi.org/10.5194/AMT-8-43-2015.

Karjalainen, P., Ntziachristos, L., Murtonen, T., Wihersaari, H., Simonen, P., Mylläri, F., Nylund, N.O., Keskinen, J., Rönkkö, T., 2016. Heavy duty diesel exhaust particles during engine motoring formed by lube oil consumption. Environ. Sci. Technol. 50 (22), 12504–12511. http://dx.doi.org/10.1021/acs.est.6b03284.

Karjalainen, P., Rönkkö, T., Simonen, P., Ntziachristos, L., Juuti, P., Timonen, H., Teinilä, K., Saarikoski, S., Saveljeff, H., Lauren, M., Happonen, M., Matilainen, P., Maunula, T., Nuottimäki, J., Keskinen, J., 2019. Strategies to diminish the emissions of particles and secondary aerosol formation from diesel engines. Environ. Sci. Technol. 53 (17), 10408–10416. http://dx.doi.org/10.1021/acs.est.9b04073.

- Kelp, M., Gould, T., Austin, E., Marshall, J.D., Yost, M., Simpson, C., Larson, T., 2020. Sensitivity analysis of area-wide, mobile source emission factors to high-emitter vehicles in los angeles. Atmos. Environ. 223, 117212. http://dx.doi.org/10.1016/ J.ATMOSENV.2019.117212.
- Knoll, M., Penz, M., Juchem, H., Schmidt, C., Pöhler, D., Bergmann, A., 2024. Large-scale automated emission measurement of individual vehicles with point sampling. Atmos. Meas. Tech. 17, 2481–2505. http://dx.doi.org/10.5194/amt-17-2481-2024.
- Kolb, C.E., Herndon, S.C., Mcmanus, J.B., Shorter, J.H., Zahniser, M.S., Nelson, D.D., Jayne, J.T., Canagaratna, M.R., Worsnop, D.R., 2004. Mobile laboratory with rapid response instruments for real-time measurements of urban and regional trace gas and particulate distributions and emission source characteristics. Environ. Sci. Technol. 38 (21), 5694–5703. http://dx.doi.org/10.1021/es030718p.
- Lau, C.F., Rakowska, A., Townsend, T., Brimblecombe, P., Chan, T.L., Yam, Y.S., Močnik, G., Ning, Z., 2015. Evaluation of diesel fleet emissions and control policies from plume chasing measurements of on-road vehicles. Atmos. Environ. 122, 171–182. http://dx.doi.org/10.1016/j.atmosenv.2015.09.048.
- Leinonen, V., Olin, M., Martikainen, S., Karjalainen, P., Mikkonen, S., 2023. Challenges and solutions in determining dilution ratios and emission factors from chase measurements of passenger vehicles. Atmos. Meas. Tech. 16, 5075–5089. http: //dx.doi.org/10.5194/amt-16-5075-2023.
- Ligterink, N., 2024. Emissiefactoren voor luchtkwaliteit en stikstofdepositie. URL https://www.tno.nl/nl/duurzaam/duurzaam-verkeer-vervoer/emissiefactorenluchtkwaliteit-stikstof/. (Accessed 29 July 2024).
- Mamakos, A., Schwelberger, M., Fierz, M., Giechaskiel, B., 2019. Effect of selective catalytic reduction on exhaust nonvolatile particle emissions of euro VI heavyduty compression ignition vehicles. Aerosol Sci. Technol. 53 (8), 898–910. http: //dx.doi.org/10.1080/02786826.2019.1610153.
- Melas, A., Selleri, T., Suarez-Bertoa, R., Giechaskiel, B., 2021. Evaluation of solid particle number sensors for periodic technical inspection of passenger cars. Sensors 21 (24), 8325. http://dx.doi.org/10.3390/S21248325.
- Ning, Z., Wubulihairen, M., Yang, F., 2012. PM, NOx and butane emissions from onroad vehicle fleets in Hong Kong and their implications on emission control policy. Atmos. Environ. 61, 265–274. http://dx.doi.org/10.1016/J.ATMOSENV.2012.07. 047
- Olin, M., Oikarinen, H., Marjanen, P., Mikkonen, S., Karjalainen, P., 2023. High particle number emissions determined with robust regression plume analysis (RRPA) from hundreds of vehicle chases. Environ. Sci. Technol. 57 (24), 8911–8920. http://dx.doi.org/10.1021/ACS.EST.2C08198.
- Pöhler, D., 2021. Heavy Duty Vehicle (HDV) NOx emission measurement with mobile remote sensing (Plume Chasing) and subsequent inspection of high emitters, study performed for Danish Road Traffic Authority. Technical Report, Danish Road Traffic Authority Færdselsstyrelsen (FSTYR), https://www.danishroadtrafficauthority.dk/Media/638350311561191389/HeavyDutyVehicle-NOxemissionmeasurementwithmobileremotesensing.pdf.
- Pöhler, D., Engel, T., Roth, U., Reber, J., Horbanski, M., Lampel, J., Platt, U., 2020. NOx RDE measurements with Plume Chasing - Validation, detection of high emitters and manipulated SCR systems. Proceedings of the 23rd Transport and Air Pollution (TAP) conference. http://dx.doi.org/10.2760/978944, 15th-17th May 2019, Thessaloniki, Greece. Part II, Karamountzou, G.(editor), Fontaras, G.(editor), Mamarikas, S.(editor), Ntziachristos, L.(editor), Publications Office, Luxembourg.
- Ropkins, K., DeFries, T.H., Pope, F., Green, D.C., Kemper, J., Kishan, S., Fuller, G.W., Li, H., Sidebottom, J., Crilley, L.R., Kramer, L., Bloss, W.J., Stewart Hager, J., 2017. Evaluation of EDAR vehicle emissions remote sensing technology. Sci. Total Environ. 609, 1464–1474. http://dx.doi.org/10.1016/j.scitotenv.2017.07.137.
- Roth, U., 2018. Optimierung und Validierung des Plume Chasing Verfahrens bei LKWs. [Bachelorthesis, University of Heidelberg].
- Saari, S., Karjalainen, P., Ntziachristos, L., Pirjola, L., Matilainen, P., Keskinen, J., Rönkkö, T., 2016. Exhaust particle and NOx emission performance of an SCR heavy duty truck operating in real-world conditions. Atmos. Environ. 126, 136–144. http://dx.doi.org/10.1016/j.atmosenv.2015.11.047.
- Shorter, J.H., Herndon, S., Zahniser, M.S., Nelson, D.D., Wormhoudt, J., Demerjian, K.L., Kolb, C.E., 2005. Real-time measurements of nitrogen oxide emissions from in-use new york city transit buses using a chase vehicle. Environ. Sci. Technol. 39 (20), 7991–8000. http://dx.doi.org/10.1021/ES048295U.

- Simonen, P., Kalliokoski, J., Karjalainen, P., Rönkkö, T., Timonen, H., Saarikoski, S., Aurela, M., Bloss, M., Triantafyllopoulos, G., Kontses, A., Amanatidis, S., Dimaratos, A., Samaras, Z., Keskinen, J., Dal Maso, M., Ntziachristos, L., 2019. Characterization of laboratory and real driving emissions of individual euro 6 light-duty vehicles fresh particles and secondary aerosol formation. Environ. Pollut. 255, 13175. http://dx.doi.org/10.1016/J.ENVPOL.2019.113175.
- Spreen, J., Kadijk, G., Vermeulen, R., Heijne, V., Ligterink, N., Stelwagen, U., Smokers, R., van der Mark, P., 2016. Assessment of road vehicle emissions: Methodology of the Dutch in-service testing programmes, TNO 2016 R11178v2. Technical Report, TNO, pp. 1–86, URL https://publications.tno.nl/publication/34622393/2csHoe/TNO-2016-R11178.pdf.
- Sugrue, R.A., Preble, C.V., Kirchstetter, T.W., 2020. Comparing the use of high- to low-cost black carbon and carbon dioxide sensors for characterizing on-road diesel truck emissions. Sensors 20 (23), 6714. http://dx.doi.org/10.3390/s20236714.
- Tong, Z., Li, Y., Lin, Q., Wang, H., Zhang, S., Wu, Y., Zhang, K.M., 2022. Uncertainty investigation of plume-chasing method for measuring on-road NOx emission factors of heavy-duty diesel vehicles. J. Hazard. Mater. 424, 127372. http://dx.doi.org/10.1016/j.jhazmat.2021.127372.
- van Eijk, E., Ligterink, N., de Ruiter, J., 2024. Emissiefactoren wegverkeer 2024 Wijzigingen in de ER en SRM emissiefactoren voor luchtkwaliteit, stikstofdepositie en klimaat. Technical Report, TNO, URL https://repository.tno.nl/SingleDoc?docId=59505.
- Vojtisek-Lom, M., Arul Raj, A.F., Jindra, P., Macoun, D., Pechout, M., 2020a. On-road detection of trucks with high NOx emissions from a patrol vehicle with on-board FTIR analyzer. Sci. Total Environ. 738, 139753. http://dx.doi.org/10.1016/J.SCITOTENV.2020.139753.
- Vojtisek-Lom, M., Zardini, A.A., Pechout, M., Dittrich, L., Forni, F., Montigny, F., Carriero, M., Giechaskiel, B., Martini, G., 2020b. A miniature portable emissions measurement system (PEMS) for real-driving monitoring of motorcycles. Atmospheric Meas. Tech. 13 (11), 5827–5843. http://dx.doi.org/10.5194/AMT-13-5827-2020.
- Wang, X., Westerdahl, D., Wu, Y., Pan, X., Zhang, K.M., 2011. On-road emission factor distributions of individual diesel vehicles in and around Beijing, China. Atmos. Environ. 45 (2), 503–513. http://dx.doi.org/10.1016/J.ATMOSENV.2010.09.014.
- Wang, H., Wu, Y., Zhang, K.M., Zhang, S., Baldauf, R.W., Snow, R., Deshmukh, P., Zheng, X., He, L., Hao, J., 2020. Evaluating mobile monitoring of on-road emission factors by comparing concurrent PEMS measurements. Sci. Total Environ. 736, 139507. http://dx.doi.org/10.1016/J.SCITOTENV.2020.139507.
- Wang, S., Zhou, B., Wang, Z., Yang, S., Hao, N., Valks, P., Trautmann, T., Chen, L., 2012. Remote sensing of NO2 emission from the central urban area of shanghai (China) using the mobile DOAS technique. J. Geophys. Res. Atmospheres 117 (13), D13305. http://dx.doi.org/10.1029/2011JD016983.
- Wen, Y., Wang, H., Larson, T., Kelp, M., Zhang, S., Wu, Y., Marshall, J.D., 2019. On-highway vehicle emission factors, and spatial patterns, based on mobile monitoring and absolute principal component score. Sci. Total Environ. 676, 242–251. http://dx.doi.org/10.1016/J.SCITOTENV.2019.04.185.
- Xiang, S., Zhang, S., Yu, Y.T., Wang, H., Shen, Y., Zhang, Q., Wang, Z., Wang, D., Tian, M., Wang, J., Yin, H., Jiang, J., Wu, Y., 2023. Evaluation of the relationship between meteorological variables and noxemission factors based on plume-chasing measurements. ACS ES T Eng. 3, 417–426. http://dx.doi.org/10. 1021/ACSESTENGG.2C00317.
- Yu, Y.S., Jeong, J.W., Chon, M.S., Cha, J., 2021. NOx emission of a correlation between the pems and sems over different test modes and real driving emission. Energies 14 (21), 7250. http://dx.doi.org/10.3390/EN14217250.
- Zavala, M., Herndon, S.C., Slott, R.S., Dunlea, E.J., Marr, L.C., Shorter, J.H., Zahniser, M., Knighton, W.B., Rogers, T.M., Kolb, C.E., Molina, L.T., Molina, M.J., 2006. Characterization of on-road vehicle emissions in the Mexico City Metropolitan Area using a mobile laboratory in chase and fleet average measurement modes during the MCMA-2003 field campaign. Atmos. Chem. Phys. 6, 5129–5142. http://dx.doi.org/10.5194/acp-6-5129-2006.
- Zhou, L., Liu, Q., Lee, B.P., Chan, C.K., Hallquist, A.M., Sjödin, A., Jerksjö, M., Salberg, H., Wängberg, I., Hallquist, M., Salvador, C.M., Gaita, S.M., Mellqvist, J., 2020. A transition of atmospheric emissions of particles and gases from on-road heavy-duty trucks. Atmospheric Chem. Phys. 20 (3), 1701–1722. http://dx.doi.org/10.5194/ACP-20-1701-2020.